Cooperative CO_2 Absorption Isotherms from a Bifunctional Guanidine and Bifunctional Alcohol

Supporting Information

Rachel Steinhardt, Stanley Hiew, Hemakesh Mohapatra, Du Nguyen, Zachary Oh,

Richard Truong, and Aaron P. Esser-Kahn

Table of Contents

I. Synthetic Procedures

Materials and Methods

Reagents (*N,N,N',N'*-tetramethyl-1,3-propanediamine, cyanogen bromide, dimethylamine, dimethylamine hydrochloride, 1,5-pentanediol, phenyl chloroformate, pyridine) were purchased from Sigma Aldrich. Silica gel (60 Å. 230-400 mesh, 40-63 μm) and calcium hydride (powder, 0-2 mm) were purchased from Sigma Aldrich. Solvents (dichloromethane, isopropanol, hexanes, ethyl acetate) were purchased from Fisher Scientific. Molecular sieves (4 Å, 4-8 mesh) were purchased from Acros Organics.

NMR spectra were acquired using a Bruker AVANCE 600 MHz spectrometer and Bruker TopSpin 3.2 software. IR (ATR) spectra were acquired using a Perkin-Elmer Spectrum Two FTIR spectrometer equipped with UATR Two accessory. High-resolution mass spectrometry was performed using an LCT Premier spectrometer.

*Synthesis of bis-cyanamide **1***

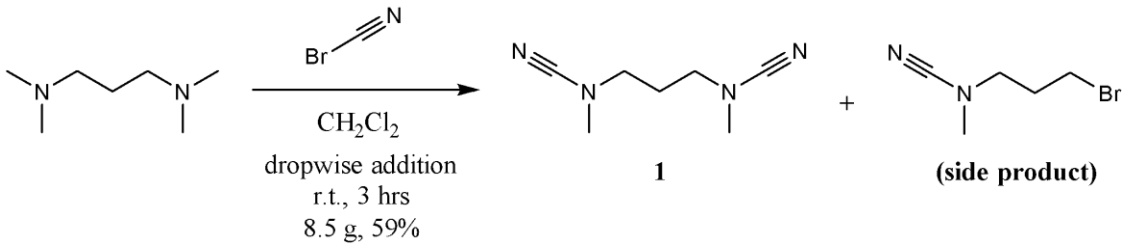

Preparation: Dichloromethane and *N,N,N',N'*-tetramethyl-1,3-propanediamine (TMPDA) were each dried by heating over CaH_2 for 3 h., followed by distillation onto 4 Å molecular sieves. ***Caution***: *cyanogen bromide hydrolyzes to hydrogen cyanide and hypobromous acid in the presence of water. The reaction should be performed using dry solvents and reagents. An appropriate quenching procedure should be used to ensure complete consumption of cyanogen bromide.*

Procedure: A 3-neck, 250 mL round-bottom flask was equipped with a stir bar and oven-dried. The middle neck was equipped with a 50 mL addition funnel and the remaining necks sealed with rubber septa. The apparatus was evacuated and backfilled with argon. Into the addition funnel was injected a solution of TMPDA (16 mL, 95 mmol, 1.0 equiv) in 35 mL dry dichloromethane. A side neck was briefly unsealed, and to the flask was added dry dichloromethane (120 mL) and cyanogen bromide (20 g, 190 mmol, 2.0 equiv). The solution was stirred until the cyanogen bromide dissolved. Using a long-needled syringe, an argon inlet was inserted through one septum into the reaction mixture while the other septum was pierced with a vent needle.

Next, the flask was lowered into a room temperature water bath. The TMPDA solution was added dropwise over 3 h. while stirring, followed by 15 min. of stirring at room temperature. Argon was bubbled through the reaction mixture continuously throughout addition of TMPDA. (The purpose of the

argon is to displace methyl bromide, a byproduct of the reaction which reacts to form tetraalkylammonium side products). The vent needle was fed to an aqueous solution of triethylamine to trap evolving methyl bromide. The apparatus was oriented so liquid from the addition funnel dropped directly into the reaction mixture. We observed that liquid running down the sides of the flask resulted in build-up of white precipitate, leading to lower yields.

To quench remaining cyanogen bromide, excess TMPDA (4 mL, 24 mmol, 0.25 equiv) was dissolved in 15 mL dichloromethane and added over 15 min. *Note: to test for remaining cyanogen bromide, a drop of the reaction mixture can be placed on wetted pH paper. The pH will appear basic (pH ~10) if the cyanogen bromide is consumed.* The resulting reaction mixture was a light-yellow solution with some of the aforementioned precipitate. The mixture was filtered to remove the precipitate, and the filtrate concentrated *in vacuo* to obtain a yellow oil.

The crude product was purified by two stages of column chromatography. In the first stage, a 1.75 inch diameter column was slurry-packed with 3 inches of silica and ethyl acetate. The crude product was diluted with 8 mL dichloromethane, loaded onto the column, and then eluted with ethyl acetate. All fractions containing bis-cyanamide **1** or the brominated side product were combined and concentrated *in vacuo*. The purpose of this first stage is to remove excess TMPDA and tetralkylammonium salts from the crude product.

In the second stage, the same sized column was slurry-packed with 7 inches of silica using 50:50 (Hex/EtOAc). The product was diluted with 5 mL ethyl acetate and loaded onto the column. The column was run with 50:50 (Hex/EtOAc) until the brominated side-product eluted, then the mobile phase changed to 20:80 (Hex/EtOAc) until **1** eluted. The fractions containing **1** were combined and concentrated by rotary evaporation to give the desired product as a clear, colorless oil (8.5 g, 56 mmol, 59%).

Developing Solvent (Hex/EtOAc)	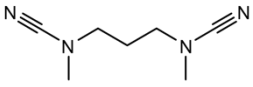	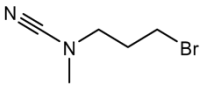
50/50	$R_f = 0.1$	$R_f = 0.7$
20/80	$R_f = 0.4$	$R_f = 0.9$

Table S1. R_f values (TLC) for bis-cyanamide **1** and brominated side-product. $KMnO_4$ stain was used to visualize both compounds.

^{1}H NMR (600 MHz, $CDCl_3$): δ 3.09 (t, *J* = 6.7 Hz, 4 H), 2.88 (s, 6 H), 1.99 (quin, *J*=6.7 Hz, 2 H)

^{13}C NMR (125 MHz, $CDCl_3$): δ 118.2, 49.9, 39.5, 25.4

IR (ATR): 2938.8 cm^{-1}, 2878.4 cm^{-1}, 2204.3 cm^{-1} **(C≡N)**

HRMS (ESI) *m/z* calcd for $[C_7H_{12}N_4 + Na]^+$: 175.0960, found 175.0953

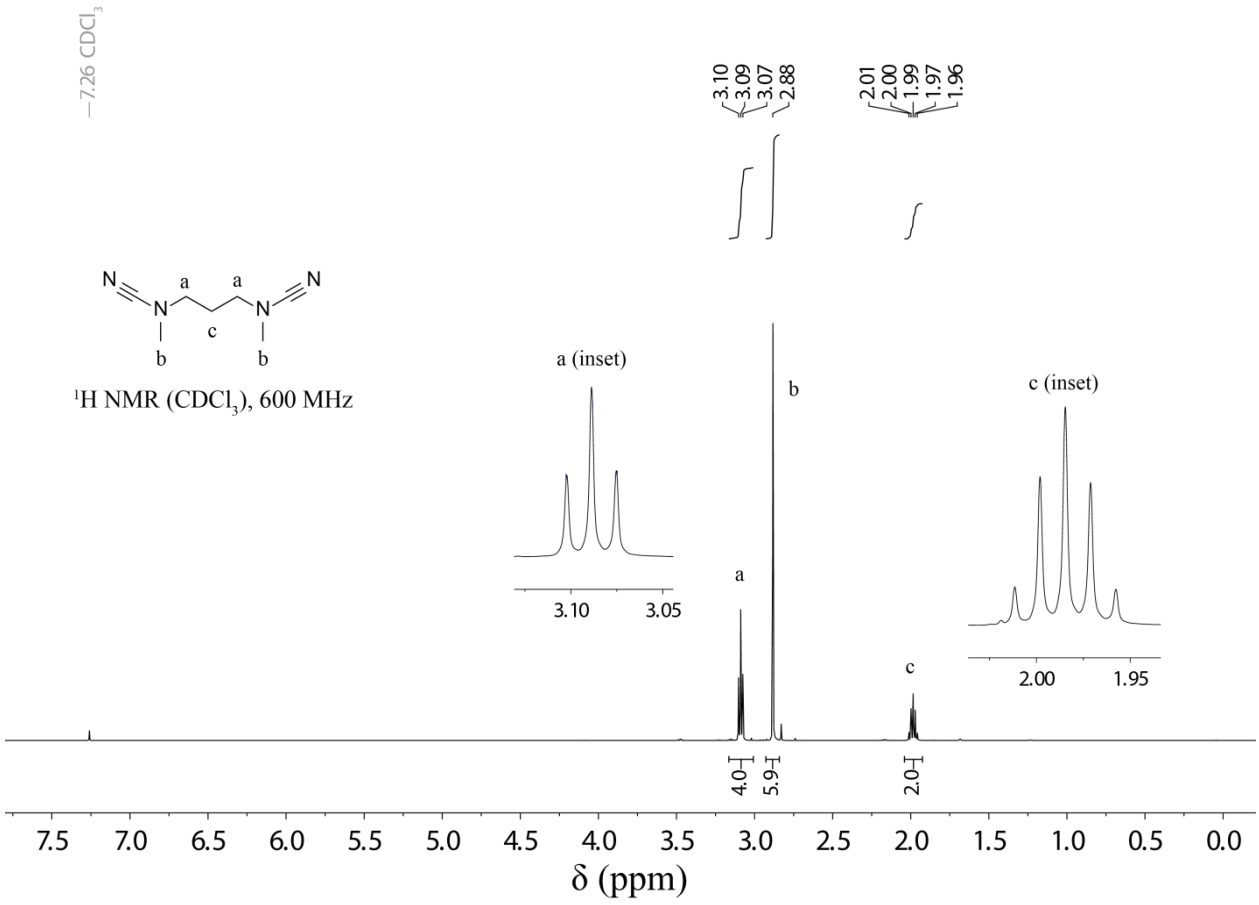
7.26 CDCl3
3.10
3.09
3.07
2.88
2.01
2.00
1.99
1.97
1.96
N
a
a
N
N
c
N
b
b
1H NMR (CDCl3), 600 MHz
a (inset)
3.10
3.05
a
b
c
c (inset)
2.00
1.95
4.0
5.9
2.0
7.5
7.0
6.5
6.0
5.5
5.0
4.5
4.0
3.5
3.0
2.5
2.0
1.5
1.0
0.5
0.0
δ (ppm)

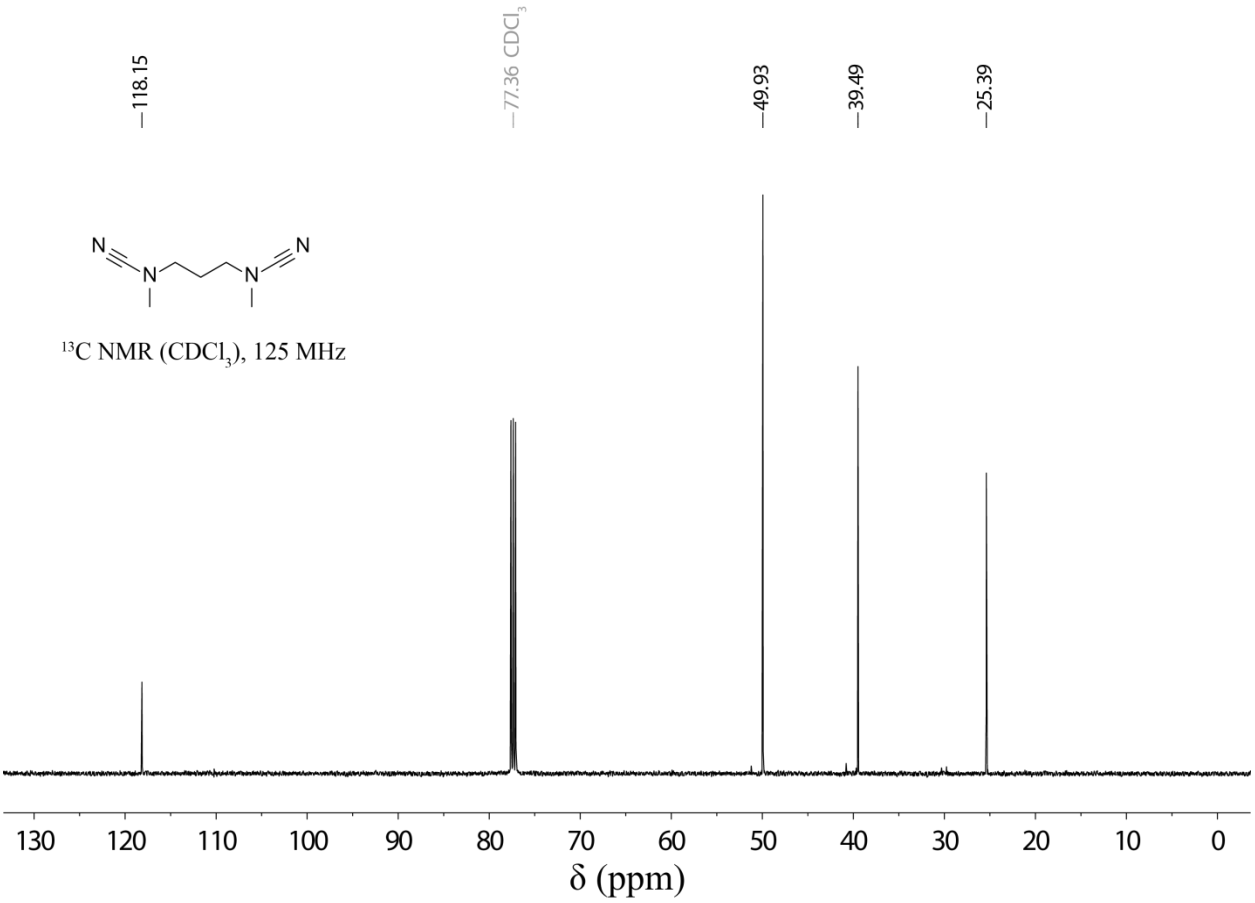
118.15
77.36 CDCl3
49.93
39.49
25.39
13C NMR (CDCl3), 125 MHz
130 120 110 100 90 80 70 60 50 40 30 20 10 0
δ (ppm)

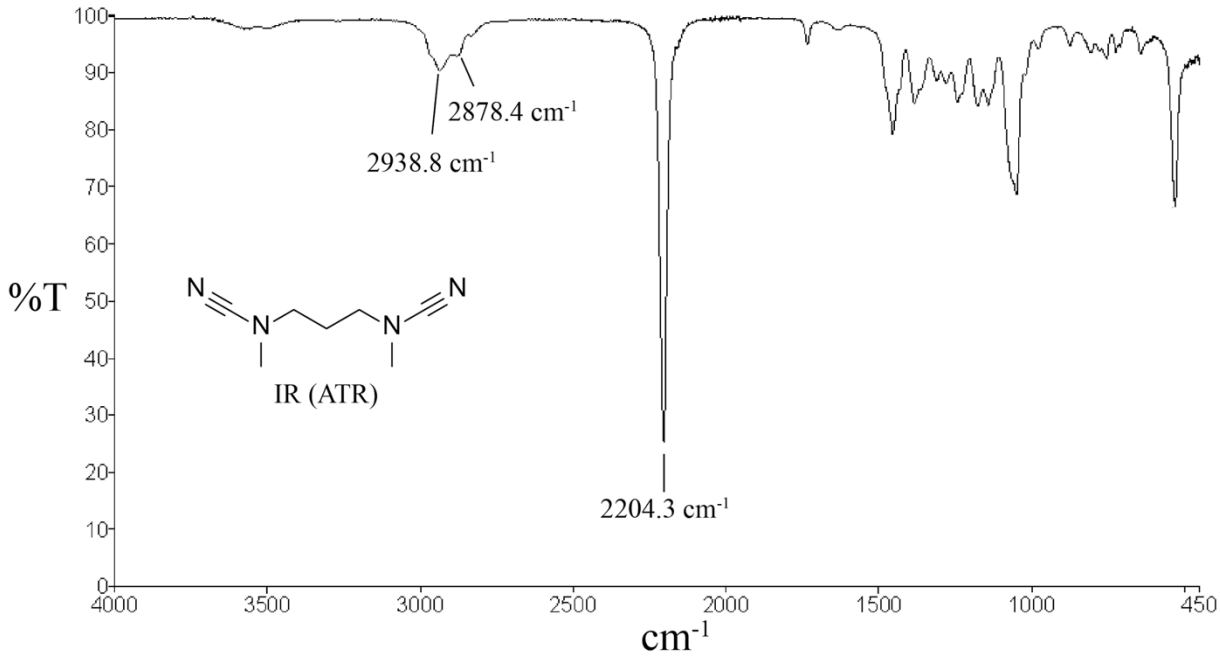
%T
2878.4 cm-1
2938.8 cm-1
2204.3 cm-1
IR (ATR)
4000 3500 3000 2500 2000 1500 1000 450
cm-1

Synthesis of bifunctional guanidine (GG)

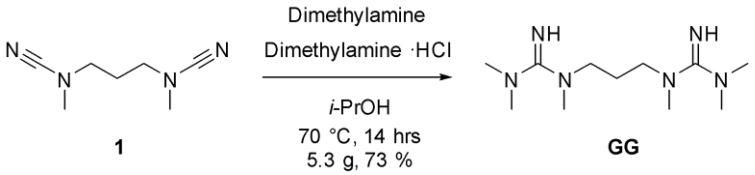

A 100 mL round-bottom flask was equipped with a stir bar and oven-dried. To the flask was added 50 mL isopropanol and the flask sealed with a rubber septum. The septum was pierced with an inlet to introduce dimethylamine gas and an outlet. While stirring, dimethylamine gas (12 g, excess) was bubbled into the solution, taking approximately 20 minutes. The amount of gas absorbed was monitored periodically by weighing the flask.

Separately, a thick-walled, pressure-safe reaction vessel (see picture on next page) was equipped with a stir bar and oven-dried. To the vessel was added bis-cyanamide **1** (4.5 g, 30 mmol, 1.0 equiv) and dimethylamine hydrochloride (7.2 g, 88 mmol, 3.0 equiv), followed by the isopropanol/dimethylamine solution. The vessel cap was tightly secured and the vessel submerged in a 70 °C oil bath while stirring. After 10 minutes of heating, the dimethylamine hydrochloride dissolved completely to give a homogenous solution. After 8 hours, the bis-hydrochloride salt of **3** began to precipitate. The reaction continued for an additional 6 hours, for a total reaction time of 14 hours. (If precipitation does not occur spontaneously, it can be facilitated by cooling the reaction mixture to room temperature, removing the cap, and re-heating the reaction mixture to 70 °C until excess dimethylamine boils off. Precipitation occurs upon cooling again to room temperature. Alternatively, the reaction mixture can be triturated with diethyl ether).

The reaction mixture was cooled to room temperature, and the vessel cap unscrewed. The precipitate was collected by filtration and washed with 60 mL ether. The precipitate was reacted with aqueous KOH (50 wt %, 50 g) and extracted with acetonitrile (3 x 75 mL). The extracted portions were combined and concentrated *in vacuo* to afford the product as a light yellow oil with residual salts. The salts were removed by re-dissolving the product in 100 mL benzene, drying over Na_2SO_4, and filtering. The solution was concentrated again *in vacuo* and dried under high vacuum for 3 h. to afford **GG** as a clear, light-yelllow oil (5.3 g, 22 mmol, 74%).

^{1}H NMR (600 MHz, CD_3CN): δ 5.24 (br, 2 H), 3.01 (t, J = 7.3 Hz, 4 H), 2.64 (s, 6 H), 2.63 (s, 12 H), 1.72-1.67 (m, 2 H)

^{13}C NMR (125 MHz, CD_3CN): δ 167.7, 49.5, 39.8, 37.1, 25.2

IR (ATR): 3316.8cm^{-1}, 2936.2cm^{-1}, 2838.9cm^{-1}, 1588.8 cm^{-1}

HRMS (ESI): *m/z* calcd for $[C_{11}H_{26}N_6 + Na]^+$: 265.2117, found 265.2113

Before Heating After Heating

Figure S1. Sealed reaction vessel containing GG reaction mixture before and after heating.

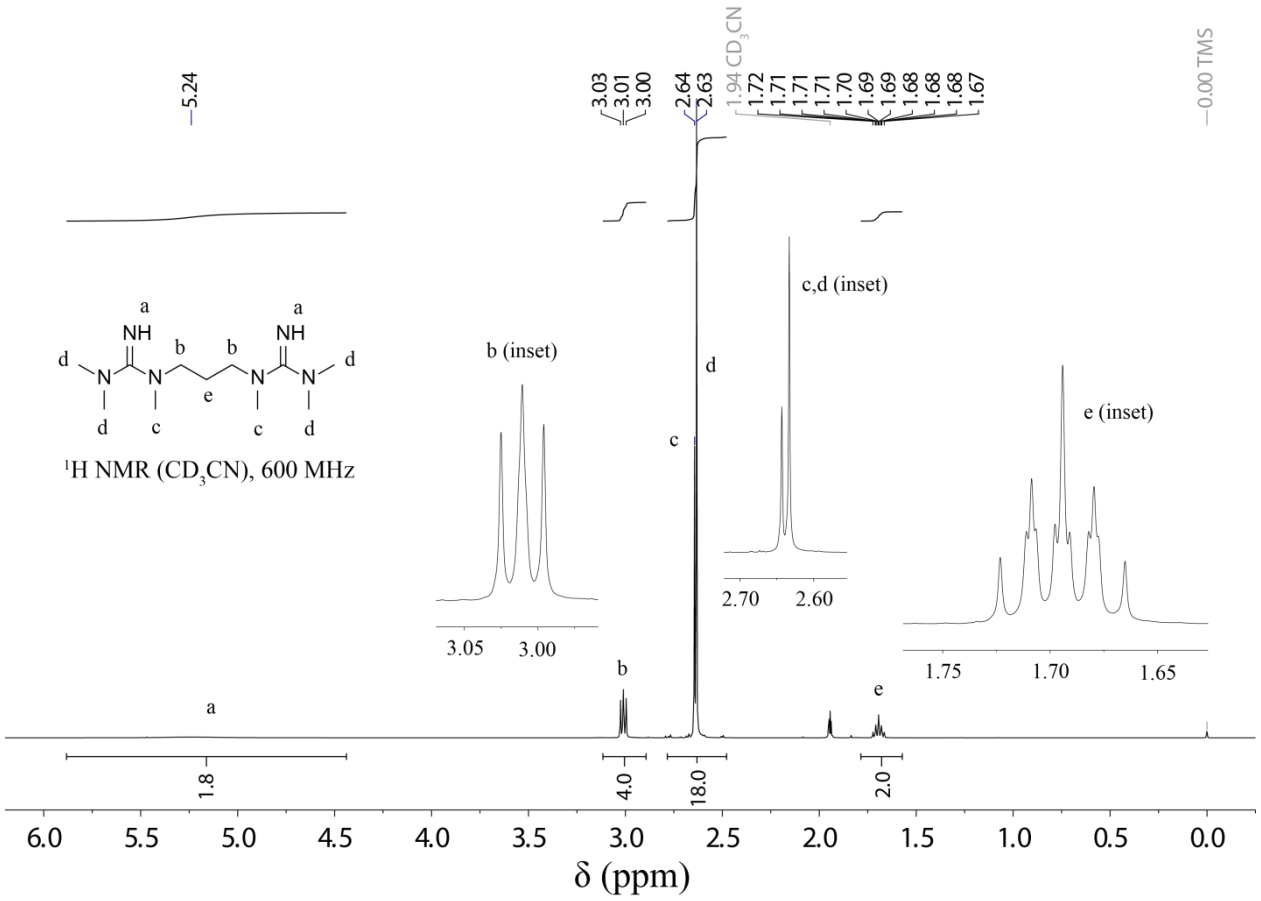
5.24
3.03
3.01
3.00
2.64
2.63
1.94 CD3CN
1.72
1.71
1.71
1.71
1.70
1.69
1.69
1.68
1.68
1.68
1.67
0.00 TMS
a
NH
b
b
NH
d
N
N
e
N
N
d
d
c
c
d
1H NMR (CD3CN), 600 MHz
b (inset)
3.05
3.00
c,d (inset)
2.70
2.60
e (inset)
1.75
1.70
1.65
a
b
c
d
e
1.8
4.0
18.0
2.0
6.0
5.5
5.0
4.5
4.0
3.5
3.0
2.5
2.0
1.5
1.0
0.5
0.0
δ (ppm)

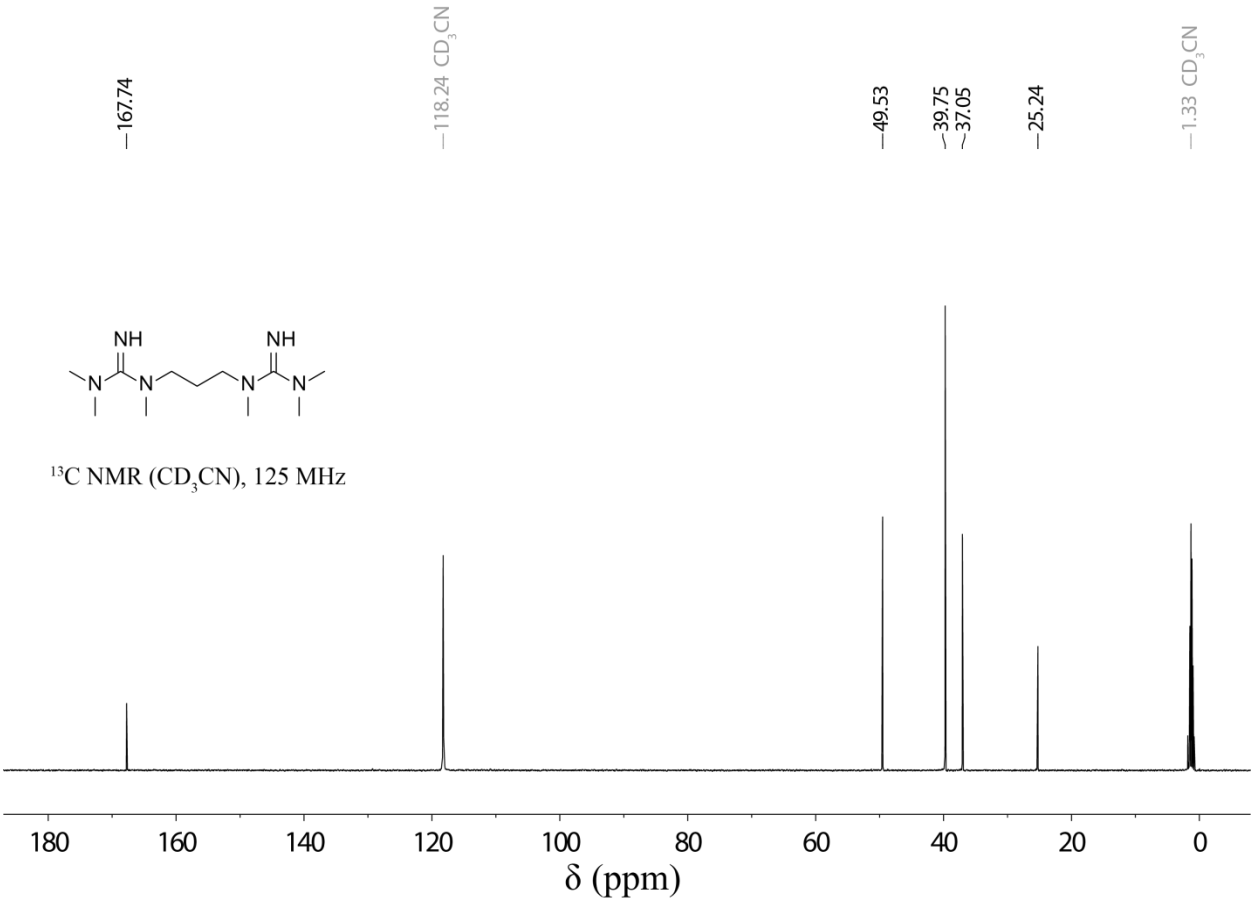
167.74
118.24 CD3CN
49.53
39.75
37.05
25.24
1.33 CD3CN
NH
NH
N
N
N
N
13C NMR (CD3CN), 125 MHz
180
160
140
120
100
80
60
40
20
0
δ (ppm)

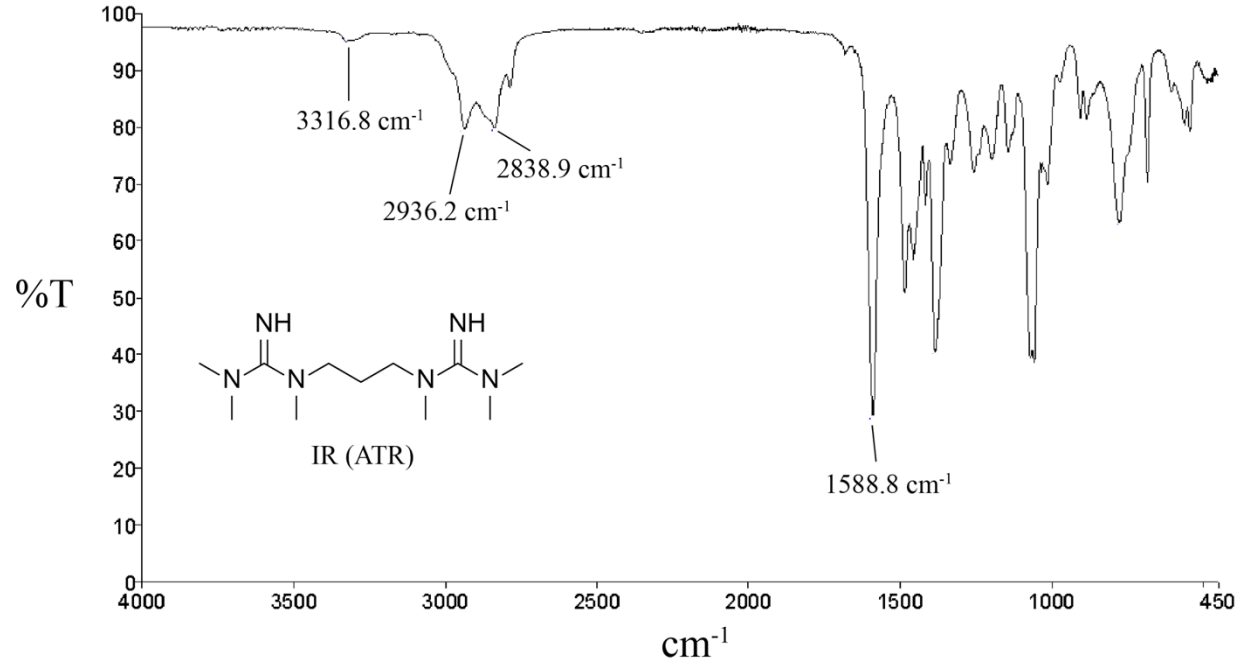
100
90
80
70
60
50
40
30
20
10
0
%T
3316.8 cm-1
2936.2 cm-1
2838.9 cm-1
1588.8 cm-1
NH
NH
N
N
N
N
IR (ATR)
4000
3500
3000
2500
2000
1500
1000
450
cm-1

Synthesis of diphenyl dicarbonate analogue of A^-A^-

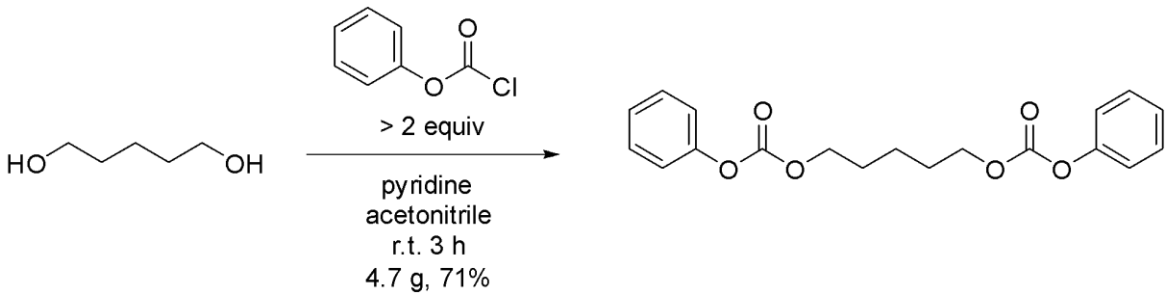

Procedure: A 100 mL round-bottom flask was equipped with a stir bar and oven-dried. To the flask was added 20 mL acetonitrile, 1,5-pentanediol (2.0 g, 19 mmol, 1 equiv), and pyridine (6.1 g, 77 mmol, 4 equiv). The flask was equipped with a 50 mL addition funnel, to which was added a solution of phenyl chloroformate (9 g, 58 mmol, 3 equiv) in 20 mL acetonitrile. The phenyl chloroformate was added dropwise over 1 h 15 min while stirring, then the mixture stirred for an additional 1 h 45 min, for a total reaction time of 3 h.

The product was purified by column chromatography. A 1.75 inch diameter column was slurry-packed with 8 inches of 90:10 (Hex/EtOAc). The crude reaction mixture was concentrated *in vacuo*, diluted with 8 mL of 70:30 (Hex/EtOAc), and loaded onto the column. The column was run with 90:10 (Hex/EtOAc) until the product eluted (R_f = 0.2). Fractions containing the product were collected and concentrated *in vacuo* to give the desired product as white crystalline needles (4.7 g, 14 mmol, 71%).

^{1}H NMR (600 MHz, CD_3CN): δ 7.44 (t, 4H), 7.30 (t, 2H), 7.22 (d, 4H), 4.27 (t, 4H), 1.80 (m, 4H), 1.55 (m, 2H)

^{13}C NMR (125 MHz, CD_3CN): δ 154.6, 152.2, 130.5, 127.0, 122.2, 69.4, 28.8, 22.7

IR (ATR): 2961 cm^{-1}, 2898 cm^{-1}, 2867 cm^{-1}, 1746 cm^{-1}

HRMS (ESI): *m/z* calcd for $[C_{19}H_{20}O_6 + Na]^+$: 367.1158, found 367.1149

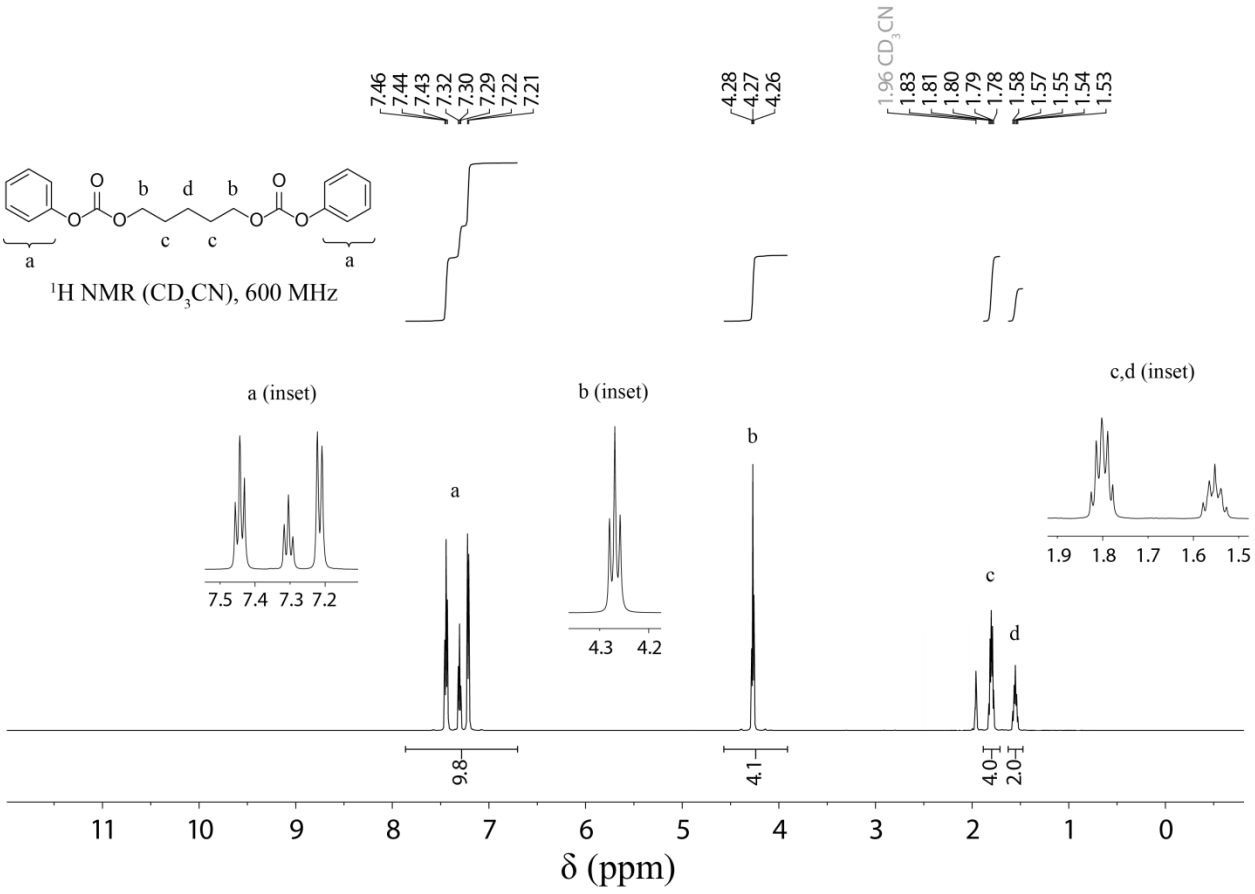
7.46
7.44
7.43
7.32
7.30
7.29
7.22
7.21
4.28
4.27
4.26
1.96 CD3CN
1.83
1.81
1.80
1.79
1.78
1.58
1.57
1.55
1.54
1.53
O
O
O
O
O
O
b
d
b
c
c
a
a
1H NMR (CD3CN), 600 MHz
a (inset)
7.5 7.4 7.3 7.2
a
b (inset)
4.3 4.2
b
c,d (inset)
1.9 1.8 1.7 1.6 1.5
c
d
9.8
4.1
4.0
2.0
11 10 9 8 7 6 5 4 3 2 1 0
δ (ppm)

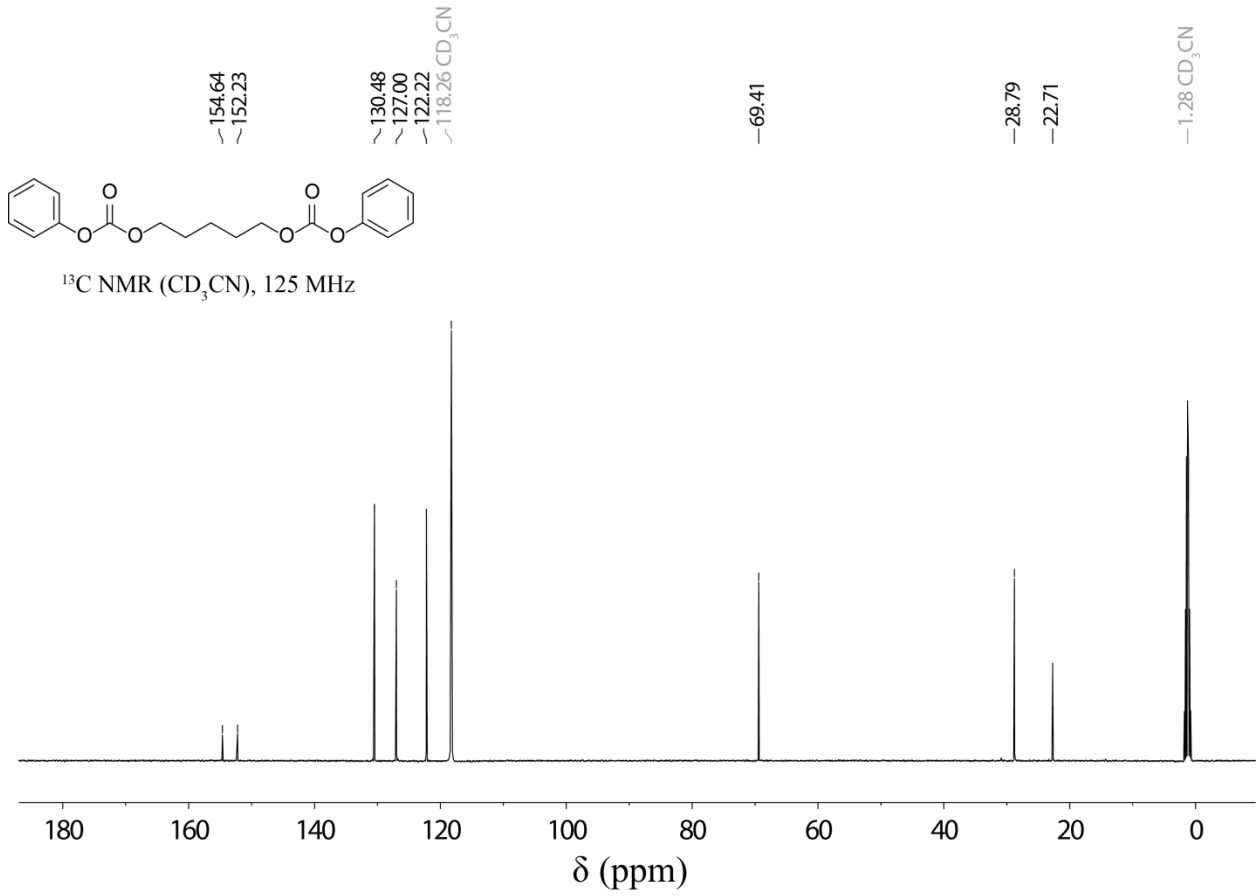
154.64
152.23
130.48
127.00
122.22
118.26 CD3CN
69.41
28.79
22.71
1.28 CD3CN
13C NMR (CD3CN), 125 MHz
180
160
140
120
100
80
60
40
20
0
δ (ppm)

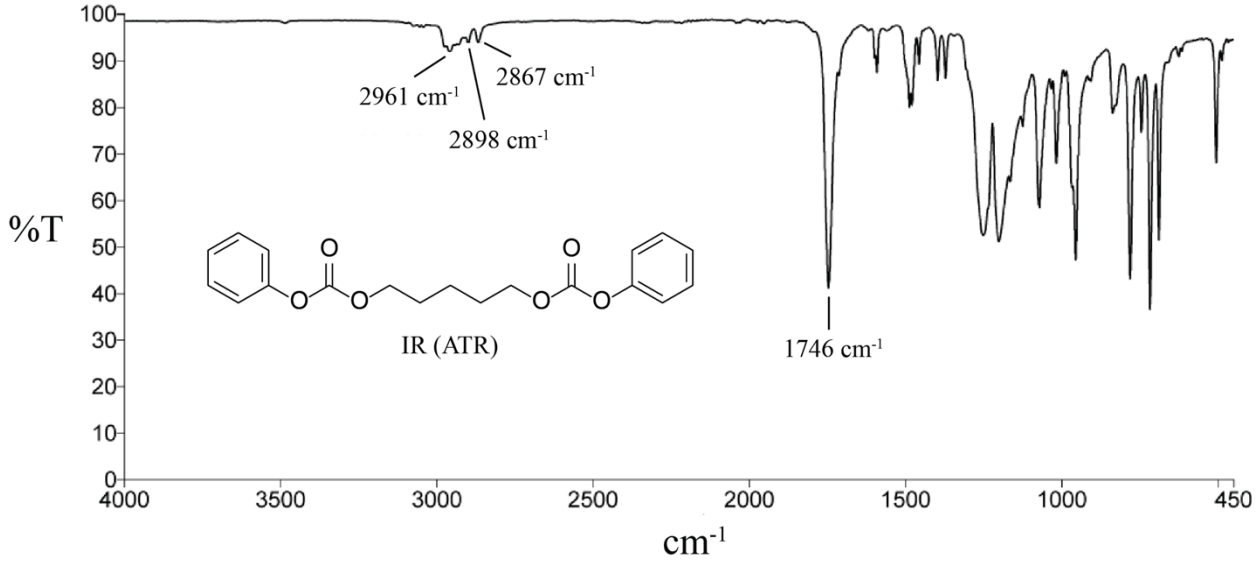
%T
2961 cm-1
2867 cm-1
2898 cm-1
1746 cm-1
IR (ATR)
4000
3500
3000
2500
2000
1500
1000
450
cm-1

Synthesis of phenyl monocarbonate analogue for A^-A

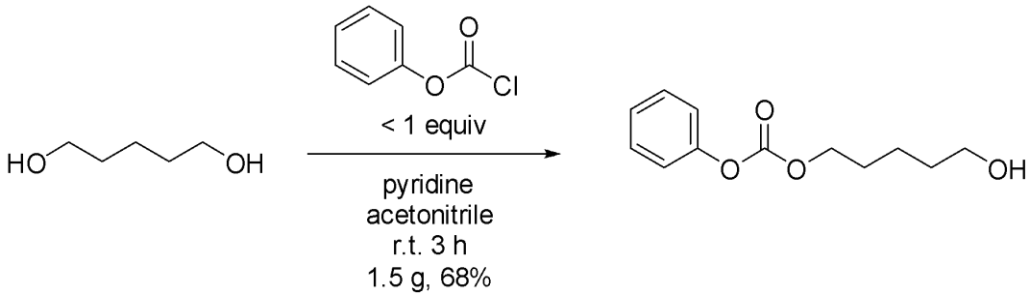

Procedure: A 100 mL round-bottom flask was equipped with a stir bar and oven-dried. To the flask was added 20 mL acetonitrile, 1,5-pentanediol (4.0 g, 38 mmol, 1 equiv), and pyridine (2.9 g, 38 mmol, 1 equiv). The flask was equipped with a 50 mL addition funnel, to which was added a solution of phenyl chloroformate (1.5 g, 10 mmol, 0.25 equiv) in 20 mL acetonitrile. The phenyl chloroformate was added dropwise over 1 h while stirring, then the mixture stirred for an additional 2 h, for a total reaction time of 3 h.

The product was purified by column chromatography. A 1.75 inch diameter column was slurry-packed with 8 inches of 80:20 (Hex/EtOAc). The crude reaction mixture was concentrated *in vacuo*, then diluted with 8 mL of 50:50 (Hex/EtOAc) and loaded onto the column. The column was run with 65:35 Hex/EtOAc until the product eluted (R_f = 0.2). Fractions containing the product were collected and concentrated *in vacuo*. The product was further dried for 5 h under high vacuum to yield a colorless oil (1.5 g, 6.6 mmol, 68%).

^{1}H NMR (600 MHz, CD_3CN): δ 7.44 (t, 2H), 7.30 (t, 1H), 7.22 (d, 2H), 4.25 (t, 2H), 3.54 (q, 2H), 2.56 (t, 1H), 1.75 (m, 2H), 1.56 (m, 2H), 1.47 (m, 2H)

^{13}C NMR (125 MHz, CD_3CN): δ 154.7, 152.2, 130.5, 127.0, 122.2, 69.7, 62.2, 33.0, 29.1, 22.8

IR (ATR): 3351 cm^{-1}, 2935 cm^{-1}, 2867 cm^{-1}, 1757 cm^{-1}

HRMS (ESI): *m/z* calcd for $[C_{12}H_{16}O_4 + Na]^+$: 247.0946, found 247.0940

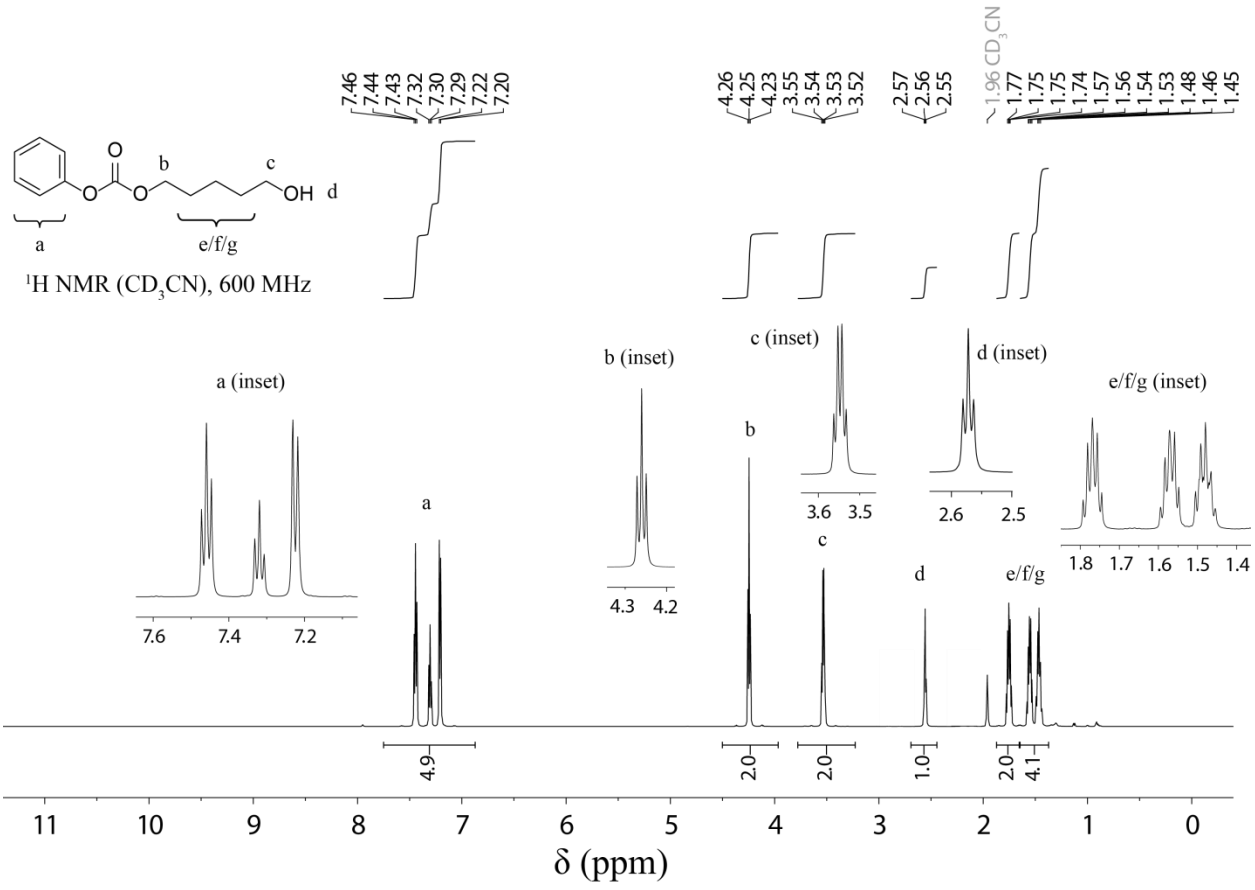
7.46
7.44
7.43
7.32
7.30
7.29
7.22
7.20
4.26
4.25
4.23
3.55
3.54
3.53
3.52
2.57
2.56
2.55
~1.96 CD3CN
1.77
1.75
1.75
1.74
1.57
1.56
1.54
1.53
1.48
1.46
1.45
O
O
O
OH
b
c
d
a
e/f/g
1H NMR (CD3CN), 600 MHz
a (inset)
b (inset)
c (inset)
d (inset)
e/f/g (inset)
a
b
c
d
e/f/g
4.9
2.0
2.0
1.0
2.0
4.1
δ (ppm)

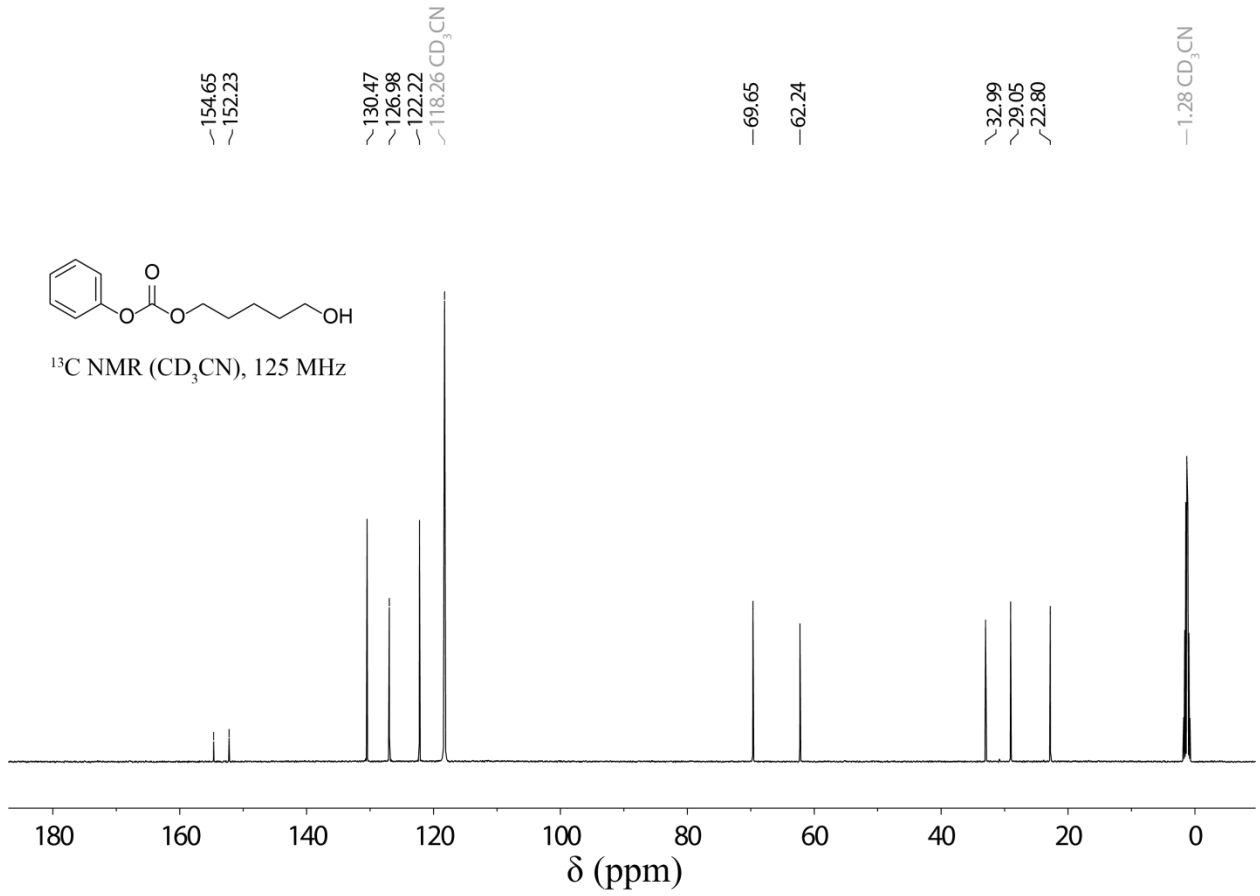
154.65
152.23
130.47
126.98
122.22
118.26 CD3CN
69.65
62.24
32.99
29.05
22.80
1.28 CD3CN
O
O
O
OH
13C NMR (CD3CN), 125 MHz
180
160
140
120
100
80
60
40
20
0
δ (ppm)

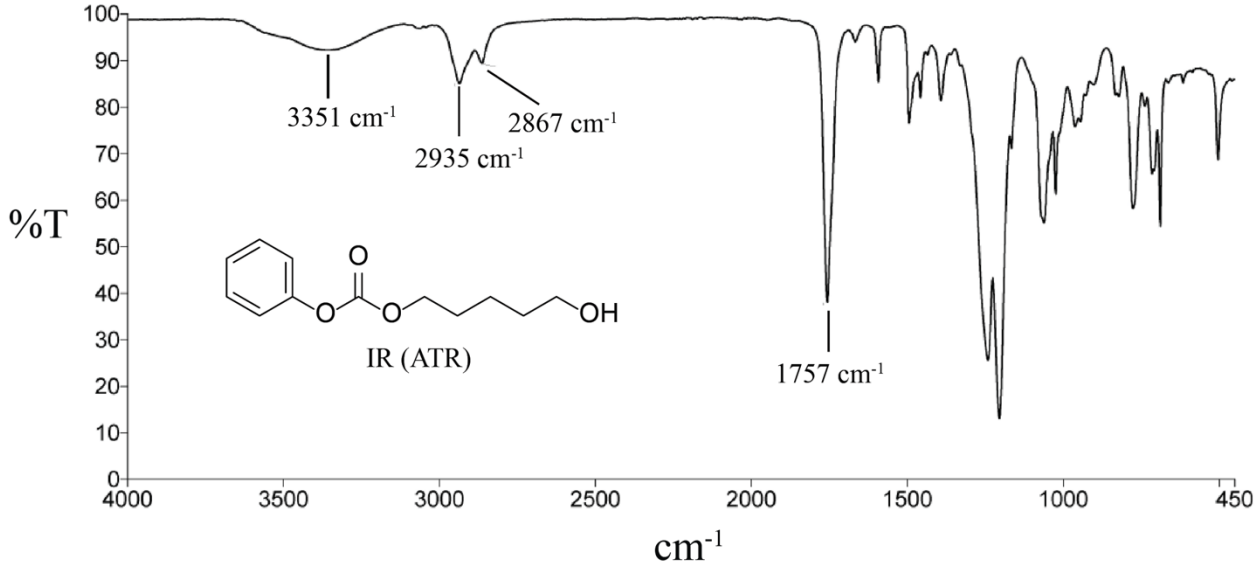
100
90
80
70
60
50
40
30
20
10
0
%T
3351 cm-1
2935 cm-1
2867 cm-1
1757 cm-1
O
O
O
OH
IR (ATR)
4000
3500
3000
2500
2000
1500
1000
450
cm-1

II. Determination of CO_2 Binding Isotherms

Carbon dioxide binding isotherms were determined using a 3Flex High Resolution, High Throughput Surface Characterization Analyzer (Micromeritics). GG and AA were dried separately over activated molecular sieves overnight. Mixtures of anhydrous GG and AA were then formulated in anhydrous solvent, and 1.0 mL of the solution added to specialized sample flasks (Micromeritics) which had been oven-dried overnight. Flasks were secured to the 3Flex instruments, and then degassed with three freeze (15 min) - pump (15 min) - thaw (15 min) cycles. After the final thaw, flasks were dosed with carbon dioxide, with constant magnetic stirring, to reach the pressures indicated in main text figure 2. ***Approximation of Flask Volume****:* Because the 3Flex requires a determination of flask volume that is reliant on exposing the contents of the sample flask to high vacuum, we used an approximation of flask + sample volume due to the vapor pressure of the liquid phase of the GG AA system. Due to the exquisite sensitivity of the instrument, this volume was determined post-measurement for each sample by inputting a volume based on the standard physical volumetric analysis of the flask and sample to two significant figures, and honing the number to four significant figures by modifying the entered flask volume such that the initial carbon dioxide absorption reading read approximately 0, and the initial slope of the measured absorption line was approximately linear. Henry's Law carbon dioxide absorption isotherms were determined for all solvents in a similar manner. The Henry's Law carbon dioxide absorption was then subtracted from the GG AA isotherms to determine the chemically-absorbed portion of carbon dioxide for each trial.

Henry's Law Plots for Solvents and Raw Data

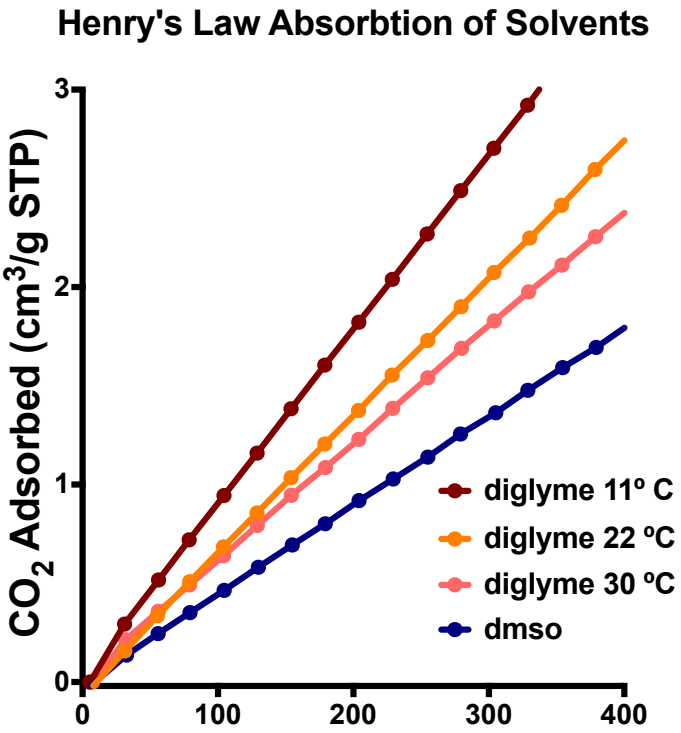

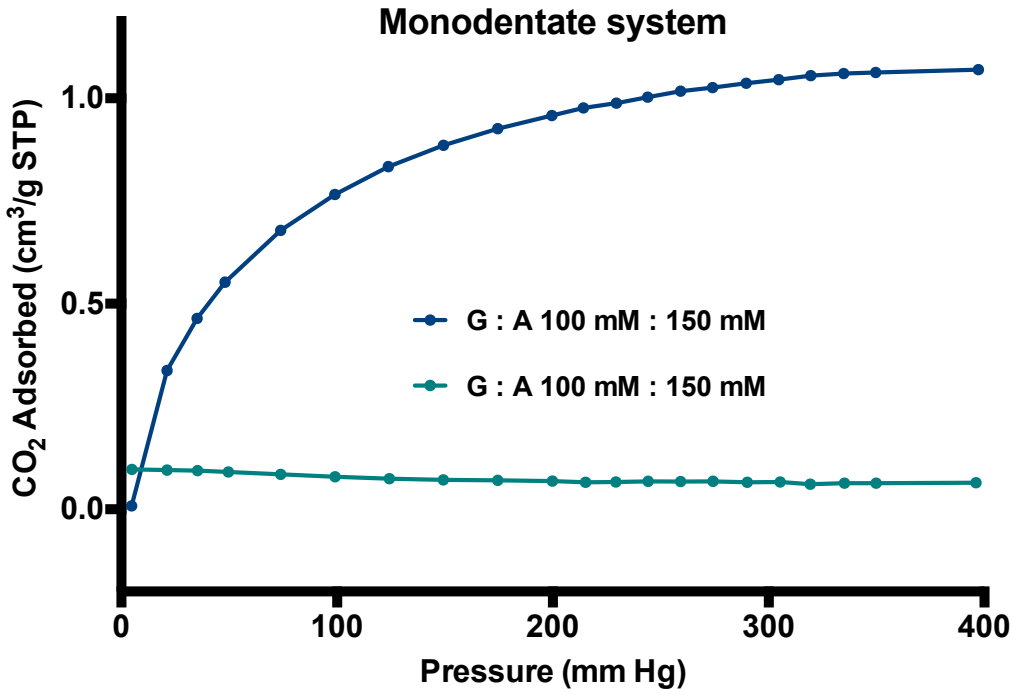
Monodentate system
1.0
0.5
0.0
CO_2 Adsorbed (cm^3/g STP)
G : A 100 mM : 150 mM
G : A 100 mM : 150 mM
0
100
200
300
400
Pressure (mm Hg)

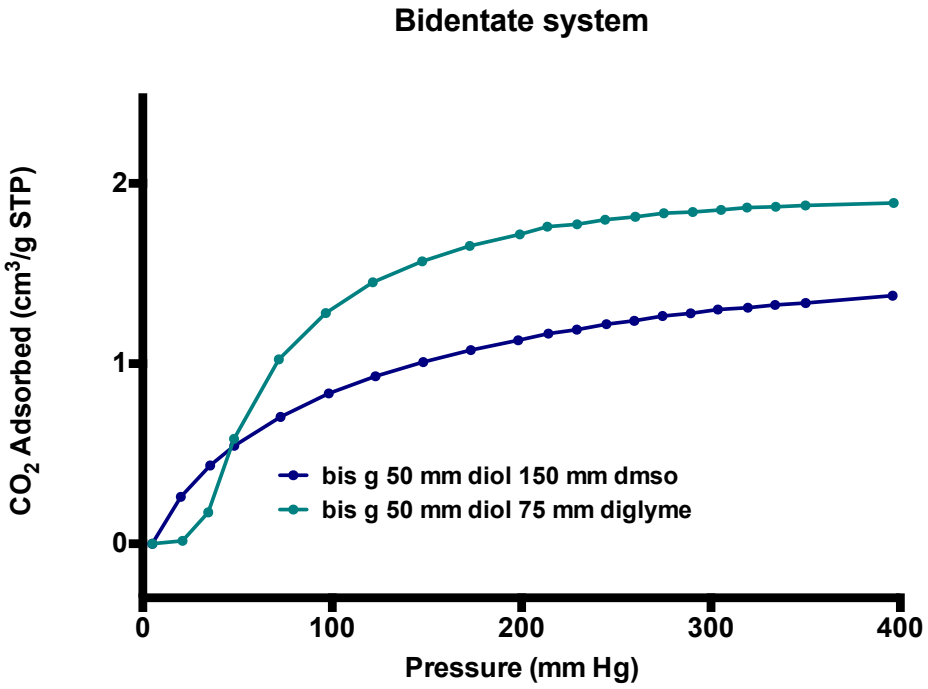
Bidentate system
2
1
0
CO_2 Adsorbed (cm^3/g STP)
bis g 50 mm diol 150 mm dmso
bis g 50 mm diol 75 mm diglyme
0
100
200
300
400
Pressure (mm Hg)

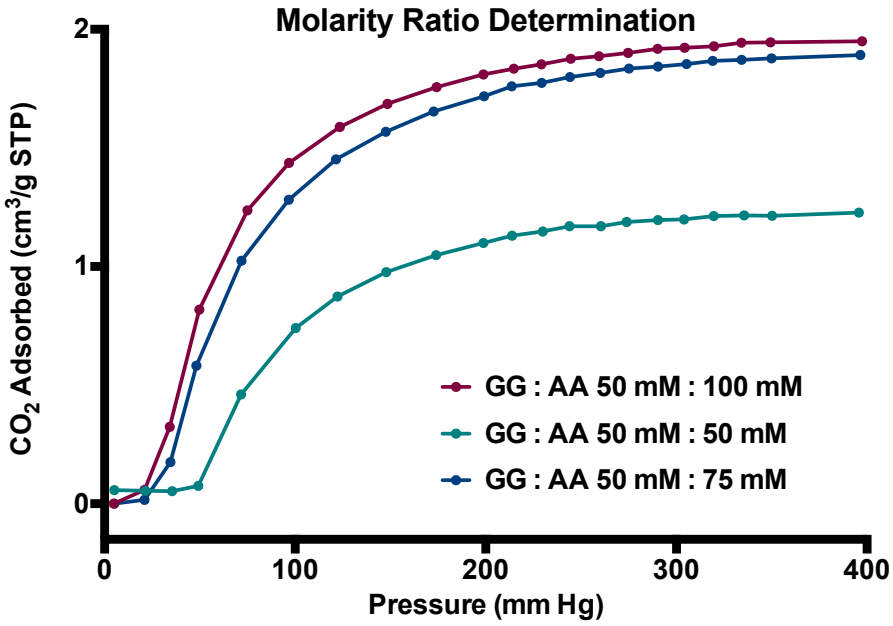

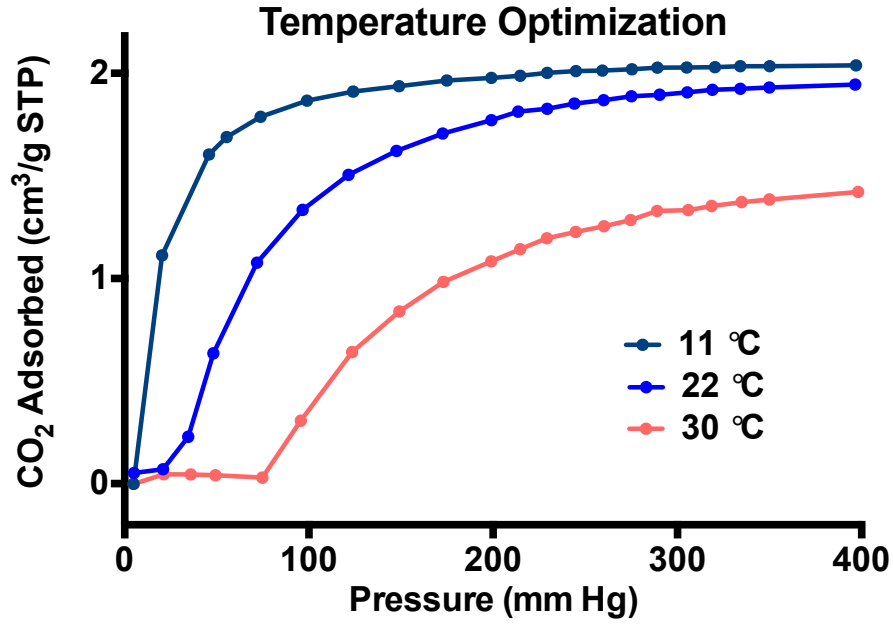

Table S2. CO_2 capacities of solutions per mL total liquid

Solution Identity	mmol CO2 per mL total liquid at 165 mbar
GG 10 mM : AA15 mM	0.0006
GG 100 mM : AA 150 mM	0.1266

GG 50 mM : AA 75 mM	0.06655
11 ºC GG 50 mM : AA 75 mM	0.08785
30 ºC GG 50 mM : AA 75 mM	0.0294
TMG 100 mM : BuOH 150 mM DMSO	0.00097
TMG 100 mM : BuOH 150 mM diglyme	0.03775
GG 50 mM : AA 75 mM DMSO	0.01029

III. NMR Species Assignments & Characterization of CO_2 Binding

To study our bifunctional system, we prepared NMR samples in which GG and AA (1,5-pentanediol) were dissolved in a co-solvent mixture of acetonitrile-d_3 and DMSO-d_6. The concentration of GG was held constant (50 mM). Depending on the experiment, the concentration of AA (50-200 mM) and/or solvent composition (20-100% DMSO-d_6) were varied (for details, see section IV).

Prior to CO_2 saturation, we observed little to no change in the ^{1}H NMR chemical shifts of AA and GG, whether present individually or as part of a mixture, indicating minimal deprotonation of the alcohol functional groups of AA by the guanidine functional groups of GG (Fig. 1). Deprotonation of alcohol by the guanidine to form alkoxide and guanidinium functional groups would cause noticeable chemical shift changes—for example the bis-hydrochloride salt of GG exhibits resonant peaks shifted significantly downfield from those of GG (Fig. 2).

Across all examined conditions, equilibration under 1 atm of CO_2 led to the formation of several new species. These included distinct monoalkylcarbonate A^-A and bisalkylcarbonate A^-A^- species. These species were in equilibrium with unreacted diol AA_f, so all three species were present simultaneously. Additionally, signals corresponding to GG all shifted downfield upon CO_2 exposure, from which we infer the formation of guandinium species, G^+G and G^+G^+. Acid-base exchange between guanidine and guanidinium functional groups likely occurs much faster than the NMR timescale, causing the signals corresponding to these species to coalesce. These signals do not resolve even upon cooling the NMR sample to -25 °C.

Fig. 3 below provides an example ^{1}H NMR spectrum for a solution of GG (50 mM) and AA (100 mM) in 20:80 DMSO-d_6/acetonitrile-d_3, before and after CO_2 exposure. Following CO_2 exposure, new, well-resolved signal appear at 3.82 ppm (H_d) and 3.74 ppm (H_b). The signal at 3.82 ppm corresponds to the protons adjacent to the newly formed alkylcarbonate functional groups of A^-A^-, while the signal at 3.74 ppm corresponds to that of A^-A. These signals at 3.82 ppm and 3.74 ppm allowed us to quantify the

ratio between A^-A and A^-A^- species (inset #1). Additionally, a second signal belonging to A^-A appears at 3.46 ppm (H_c), but overlaps with a signal belonging to the unreacted AA_f (H_a). Under certain conditions (for example: GG, 12.5 mM and AA, 25 mM in 100% DMSO-d_6) these overlapping resonances become at least partially resolved (inset #2).

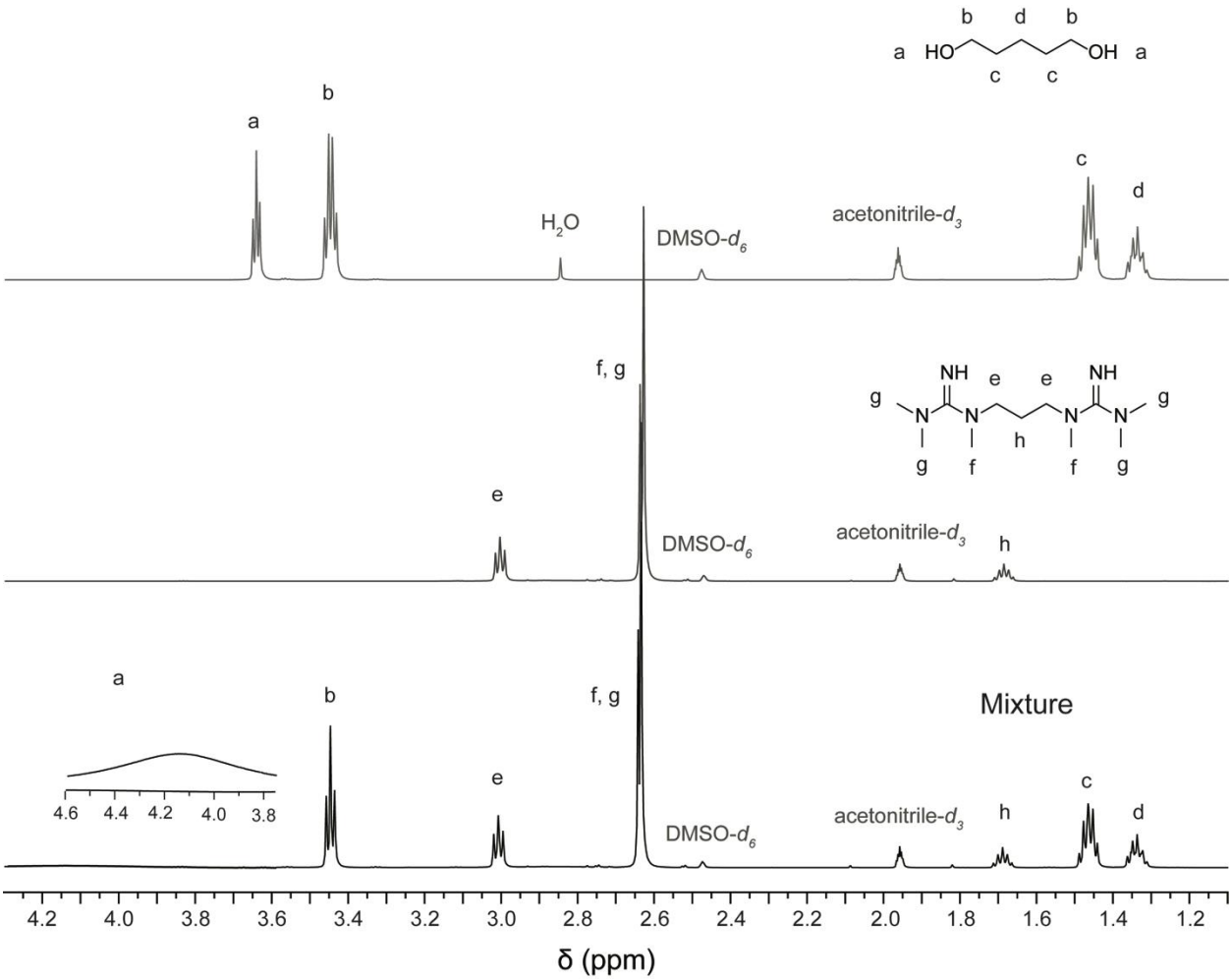

Figure S2: ^{1}H NMR spectra for AA and GG individually and as a mixture. (NMR solvent: 20/80 (v/v) DMSO-d_6/acetonitrile-d_3). Note: peak labels a–h refer to the chemical shifts of the methylene protons labeled with the corresponding letters in the chemical structure insets.

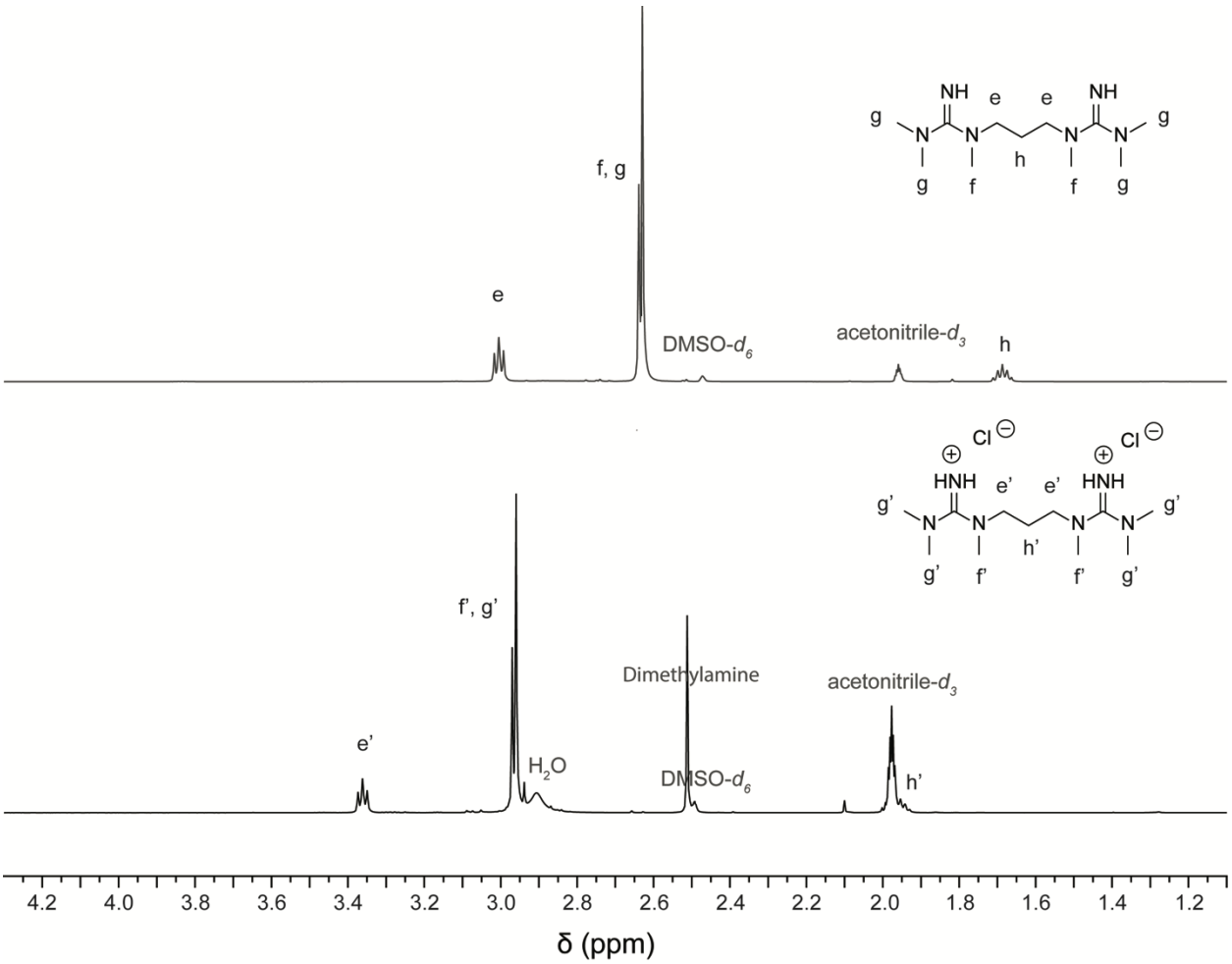

Figure S3. ^{1}H NMR signals corresponding to the bis-hydrochloride salt of *GG* (e', f', g', and h') are all shifted downfield relative to those of *GG* (e, f, g, and h). (The ^{1}H NMR spectrum of the bis-hydrochloride salt contains some dimethylamine HCl as an impurity, which co-precipitates with the salt during isolation. Some water is also present).

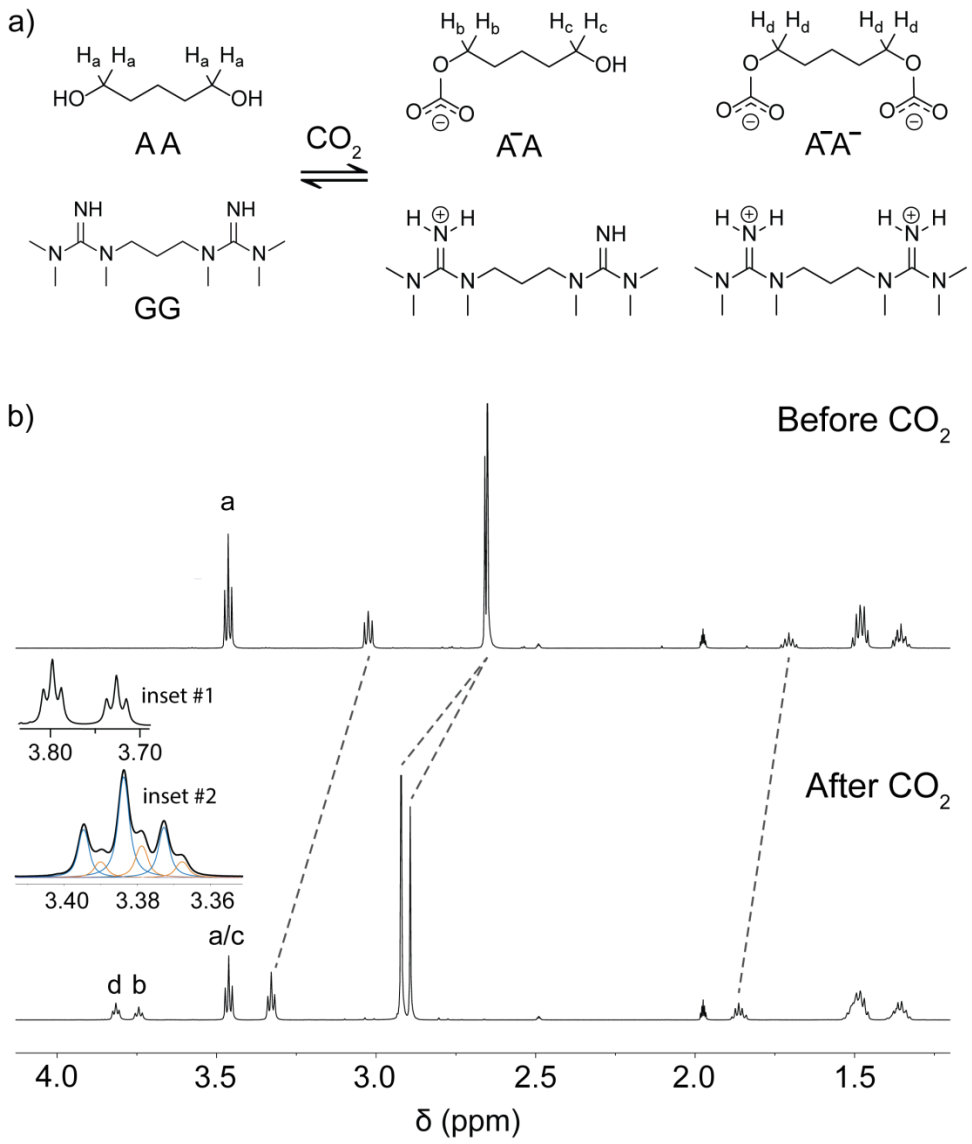

Figure S4. a) Species formed after exposure to CO_2. b) ^{1}H NMR spectra before and after 1 atm CO_2 exposure. Dashed lines correspond to GG or resulting guanidinium species. Inset #1: close-up of signals corresponding to H_d and H_b; Inset #2: H_a and H_c partly resolved under certain solvent and concentration conditions.

Our species assignments were further supported by ^{13}C NMR and ^{1}H Total Correlation Spectrosocopy (^{1}H TOCSY) experiments. As with the ^{1}H NMR spectrum, the ^{13}C NMR spectrum showed the appearance of several new signals following CO_2 exposure, consistent with the formation of A^-A and A^-A^- species (Fig. 4). Before exposure, seven signals were found between 20 and 65 ppm corresponding to aliphatic carbons, of which three belong to AA and four belong to GG. After CO_2 exposure, eight additional signals appear in this region. This number accounts for the five new signals expected from A^-A and the three new signals expected from A^-A^-. Additionally, two new signals appear between 157 ppm and 159 ppm, accounting for the sp^2-hybridized carbons of the newly formed alkylcarbonate functional

groups, one each from $A^{-}A^{-}$ and $A^{-}A$. The ^{13}C NMR acquisition and processing parameters are provided in Table S3.

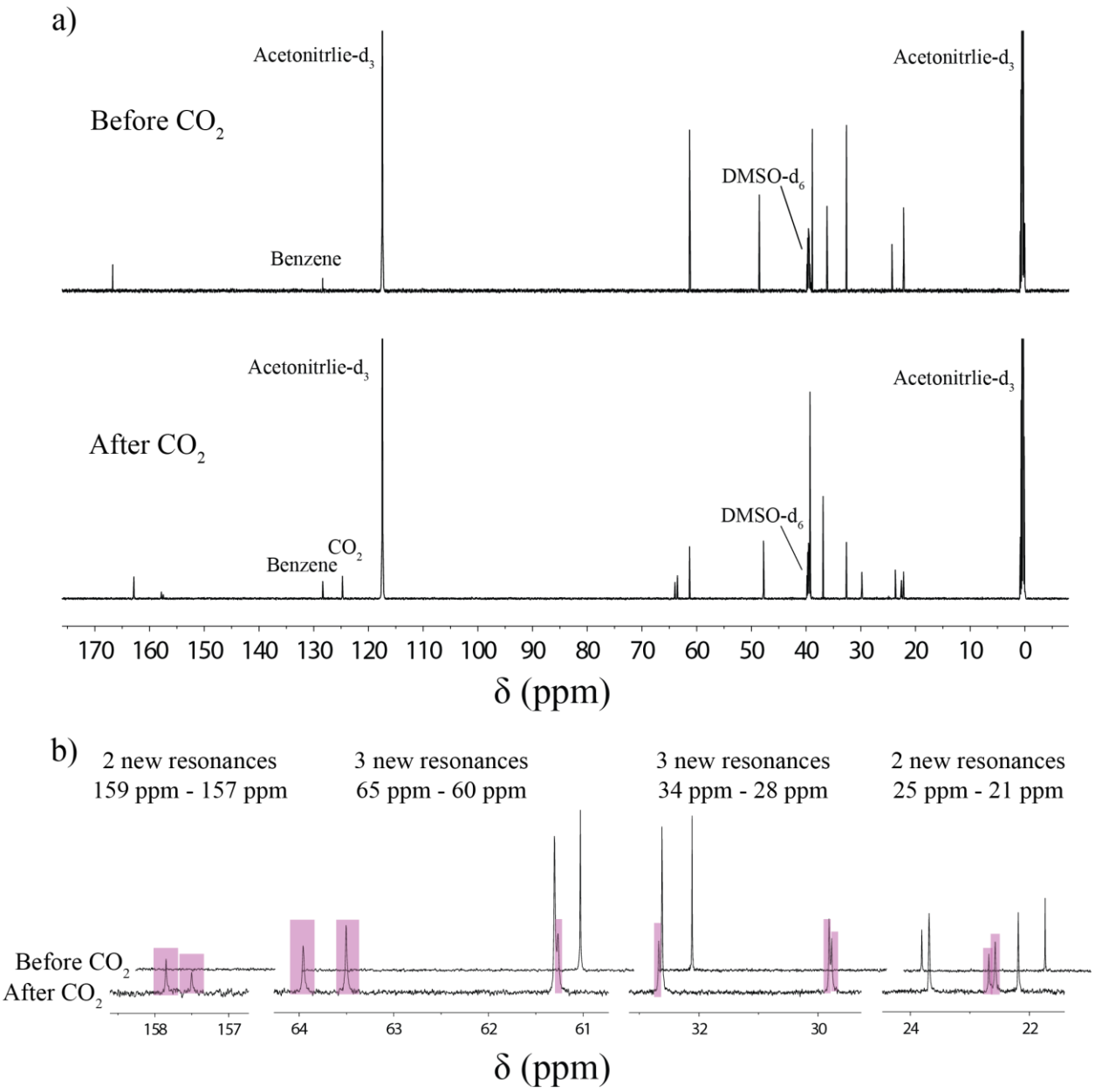

Figure S5. A) ^{13}C NMR spectra for the mixture of GG and AA, before and after CO_2 exposure. (Signal at 128.4 ppm is from residual benzene used to isolate GG). B) Magnification of key portions of the spectra shown in A), with new peaks highlighted.

^{13}C NMR Acquisition Parameters
(^{13}C with ^{1}H decoupling)

Pulse program (pulprog)	zgdc30
Number of scans (NS)	1024
FID size (TD)	65536
Sweep width (SW)	240.07 ppm / 36232 Hz
Transmitter frequency offset (O1)	
^{13}C Nucleus	110.00 ppm / 16599 Hz
^{1}H Nucleus	5.000 ppm / 3001 Hz
Acquisition Time (s)	0.9044 s
Dwell time (DW)	13.800 μs
FID resolution (FIDRES)	1.1057 s
Filter Width (FW)	625000 Hz
Acquisition Mode (AQ_mod)	DQD
Temperature	25 °C

Processing Parameters

Apodization	Exponential (1.00 Hz)
Phase correction	Manual PHO and PH1 correction; pivot point at 117 ppm
Baseline correction	3° Berstein polynomial

Table S3. Acquisition and processing parameters for ^{13}C NMR.

^{1}H TOCSY was used to check for a correlation between the signals at 3.74 ppm and 3.46 ppm (Fig. 5). Because both of these signals were assigned to $A^{-}A$, they should reside in the same spin system and give rise to a total correlation signal. In contrast, there should be no correlation between either of these signals with the signal at 3.82 ppm, as this resonance was assigned to $A^{-}A^{-}$. Based on this reasoning, we performed parallel ^{1}H-TOCSY experiments. We found that the standard two-dimensional TOCSY experiment led to a large artifact resulting from the methyl resonances at 2.92 ppm, so we performed the TOCSY experiment in a one-dimensional format, in which selective irradiation of a chosen resonance allowed us to observe other resonances in the same spin system. Following irradiation of the $A^{-}A$ resonance at 3.74 ppm (H_b), we observed a total correlation signal primarily from the resonances at 3.46 ppm (H_c) and from the methylene resonances at 1.35 ppm and 1.48 ppm. In contrast, irradiation of the $A^{-}A^{-}$ resonance at 3.82 ppm (H_d) showed a much weaker correlation with the resonance at 3.46 ppm, suggesting that these two resonances belong to different species. Taken together, the ^{1}H NMR, ^{13}C NMR, and ^{1}H TOCSY spectra are consistent with our species assignments. The ^{1}H TOCSY acquisition and processing parameters are provided in Table 2.

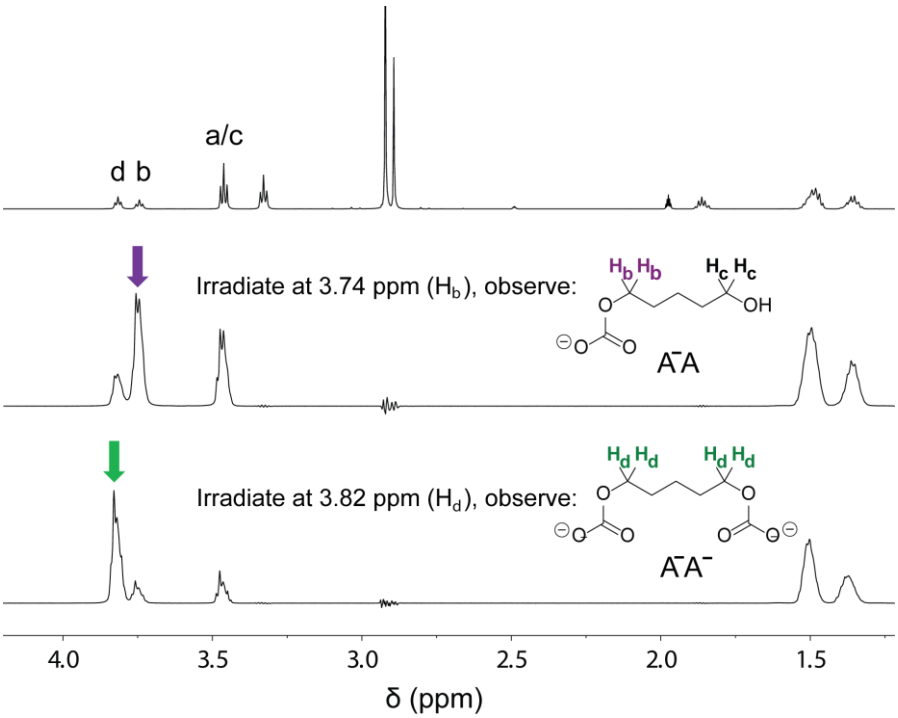

Figure S6. One-dimensional, ^{1}H TOCSY spectra for *GG* (50 mM) and *AA* (100 mM) in 20% DMSO-d_6, following CO_2 exposure. Note: peak labels a–d refer to the chemical shifts of the methylene protons labeled with the corresponding letter subscripts in the chemical structure insets.

^{1}H TOCSY Acquisition Parameters

(1D ^{1}H TOCSY)

Pulse program (pulprog)	selmlgp.2
Mixing time (D9)	0.0800 s
Number of scans (NS)	256
FID size (TD)	98074
Sweep width (SW)	12.80 ppm / 7684 Hz
Transmitter frequency offset (O1)	3.824 ppm / 2295 Hz
Acquisition Time (AQ)	6.3813 s
Dwell time (DW)	65.067 µs
FID resolution (FIDRES)	0.1567 s
Filter Width (FW)	125000 Hz
Acquisition Mode (AQ_mod)	DQD
Temperature	25 °C

Processing Parameters

Apodization	Exponential (0.30 Hz)
Phase correction	Manual PHO and PH1 correction; pivot point at 2.9 ppm
Baseline correction	Segments; anchor points at 0.5, 2.2, 5.0, and 11.0 ppm

Table S4. Acquisition and processing parameters for 1D ^{1}H TOCSY.

As a final confirmation of our species assignments, we synthesized isolable phenyl carbonate analogues of both $A^{-}A$ and $A^{-}A^{-}$. A mixture comprising these analogues plus AA and GG was prepared, and the ^{1}H NMR spectrum for this mixture compared to that obtained for the bidentate system following CO_2 exposure (Fig. 6). The two spectra closely resemble each other. For the alkylcarbonate species formed from CO_2 binding, the protons adjacent to carbonate functional groups appear downfield at 3.74 ppm ($A^{-}A$) and 3.82 ppm ($A^{-}A^{-}$); protons adjacent to the unreacted alcohol functional groups of $A^{-}A$ and AA appear near 3.46 ppm (overlapping). For the phenyl carbonate analogues, these protons adjacent the carbonate group appear somewhat farther downfield, at 4.22 ppm and 4.25 ppm; protons adjacent to the unreacted alcohol functional group of the phenyl monocarbonate analogue and AA appear at 3.48 ppm and 3.45 ppm, respectively (partly overlapping).

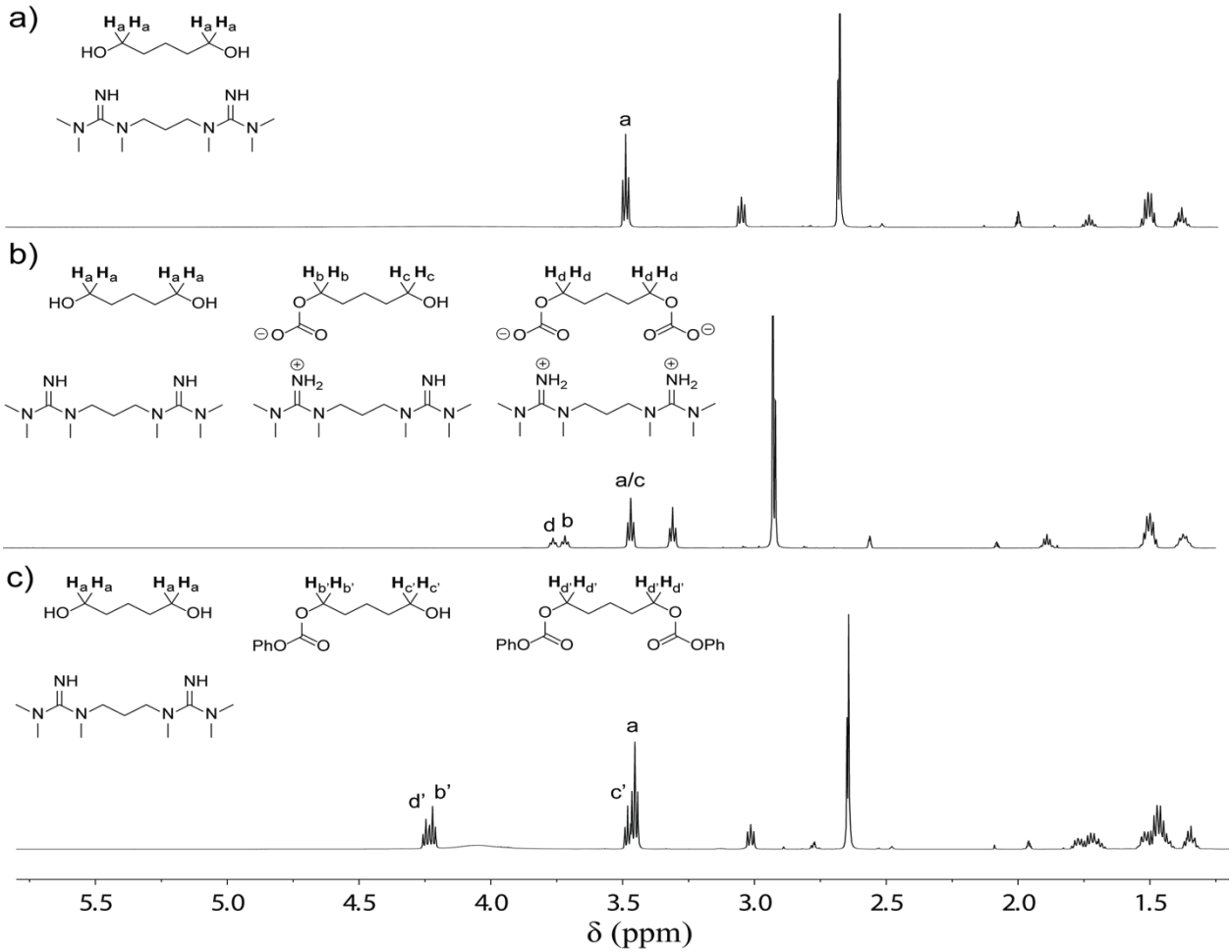

Figure S7. NMR spectra comparing $A^{-}A$ and $A^{-}A^{-}$ to their isolable phenyl carbonate analogues. a) AA and GG before CO_2 exposure. b) AA and GG after CO_2 exposure. c) Mixture of AA, GG, and the phenyl carbonate analogues

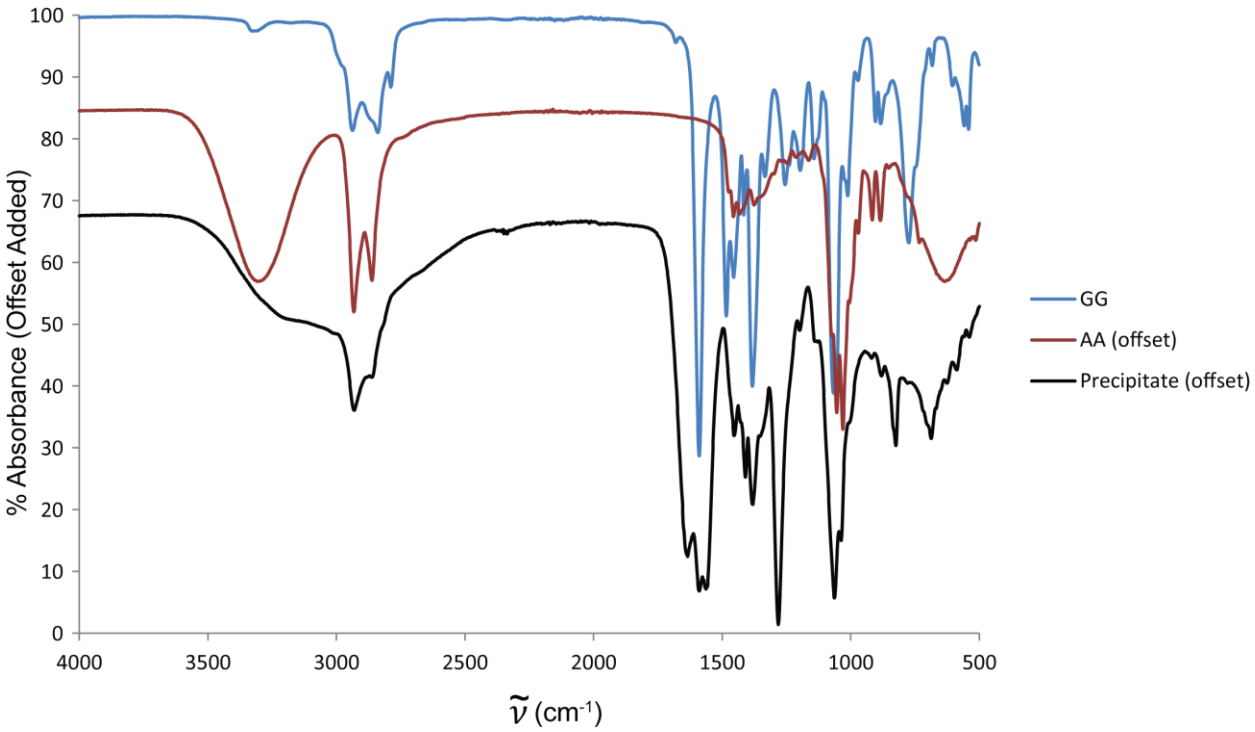

Figure S8. Infrared spectra (ATR-IR) of GG, AA, and the precipitate formed following CO_2 binding.

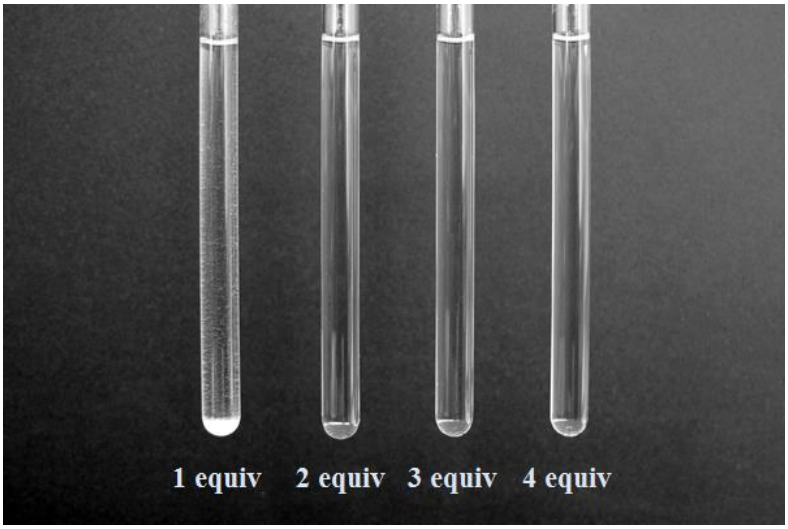

Figure S9. During our NMR experiments, we observed the formation of a white precipitate when the initial concentrations of AA or GG were equal. This observation is consistent with oligomerization pathways expected to be favored under these equimolar conditions. The precipitate disappears after addition of an extra equivalent of either AA or GG.

IV. ^{1}H NMR Titration Experiments

Materials: NMR solvents were obtained from Cambridge Isotope Labs and dried over 4Å molecular sieves before use. 1,5-pentanediol (Alfa Aesar) was distilled over CaH_2. Bidentate guanidine GG was dried under high vacuum at room temperature for 3 h. Samples were prepared in J. Young style NMR tubes (Norell, Catalog #: S-5-600-VT-8).

Solvent Titration

A series of samples were prepared with varying solvent composition, ranging from 20-100% DMSO-d_6 in 10% increments (acetonitrile-d_3 was used as the co-solvent). For all samples, the concentrations of GG (50 mM) and AA (100 mM) were held constant. To ensure accurate sample concentrations, stock solutions were prepared (GG, 0.5 M in DMSO-d_6; AA, 1.0 M in DMSO-d_6), then the appropriate amount dispensed into the NMR tube using a 100 µL syringe (Hamilton). The NMR tubes were connected to a Schlenck line, subjected to 4-5 freeze-pump-thaw cycles to remove dissolved gases, then backfilled with CO_2. The samples were equilibrated at 22 ± 2 °C under 1 atm CO_2 for ten minutes with continuous agitation. Spectra were acquired with an AVANCE 600 MHz spectrometer at 25 ± 0.5 °C using Bruker TopSpin 3.2 software. A long duty cycle, including extended delay (D1 = 12.5 s) and acquisition time (AQ = 10 s), was used to ensure full nuclear relaxation. Spectra were processed using MestRe NOVA v. 8.1 sofatware. NMR acquisition and processing parameters for the solvent titration are listed in Table 3.

^{1}H NMR Acquisition Parameters	
Pulse program (pulprog)	zg30
Delay time (D1)	12.5 s
Number of scans (NS)	8
FID size (TD)	98074
Sweep width (SW)	12.82 ppm / 7692 Hz
Transmitter frequency offset (O1)	5.61 ppm / 3369 Hz
Acquisition Time (AQ)	10 s
Dwell time (DW)	65.000 µs
FID resolution (FIDRES)	0.1 s
Filter Width (FW)	125000 Hz
Acquisition Mode (AQ_mod)	DQD
Temperature	25 °C
Processing Parameters	
Apodization	Exponential (0.30 Hz)
Phase correction	Manual PHO and PH1 correction; pivot point at 2.9 ppm
Baseline correction	Segments; anchor points at 0.5, 2.2, 5.0, and 11.0 ppm

Table S5. Acquisition and processing parameters for solvent titration ^{1}H NMR

After the NMR spectra were recorded, the relative ratio between A^-A^- and A^-A was determined at each solvent composition. This was done by finding the relative integration of these species, using the well-resolved resonances between 3.6 ppm and 3.9 ppm. While the chemical shift for these resonances changed with solvent composition, the resonance belonging to A^-A^- was always observed downfield to that belonging to A^-A. The ratio between the two species $\frac{A^-A^-}{A^-A}$ was calculated, then plotted as a function of solvent composition (Fig. 9).

Next, the ratio $\frac{A^-A^-}{A^-A}$ expected for a non-cooperative (no proximity effect) system was calculated. For a non-cooperative system, the ratio should be statistically determined and dependent only on the fraction of alcohols converted to alkylcarbonates. For example, consider a system in which 40% of the alcohols are converted to alkylcarbonates. There is a $(0.4)(0.4) = 0.16$ probability that both the alcohols of AA are both converted to alkylcarbonates (A^-A^-), a $(1-0.4)(1-0.4) = 0.36$ probability that neither alcohol is converted to an alkylcarbonate (AA), and a $(0.4)(1-0.4) + (1-0.4)(0.4) = 0.48$ probability that just one of the alcohols is converted to an alkylcarbonate (A^-A). The ratio $\frac{A^-A^-}{A^-A}$ would then be $\frac{0.16}{0.48} = 0.33$. In general, if the fraction of alcohols converted to alkylcarbonates is p, then the probability of obtaining A^-A^- is p^2 and the that of obtaining A^-A is $2(p)(1-p)$. The ratio $\frac{A^-A^-}{A^-A}$ is then $\frac{p^2}{2(p)(1-p)}$ or simply $\frac{p}{2(1-p)}$. Experimentally, p was determined by integrating signals falling between 3.6 ppm to 3.9 ppm (corresponding to protons adjacent the alkyl carbonate group), then dividing this value by the combined integration of resonances falling between 3.35 ppm to 3.9 ppm (corresponding to the protons adjacent an alkylcarbonate plus those adjacent an unreacted alcohol).

The experiment was repeated in triplicate to determine the standard error associated with the value $\frac{A^-A^-}{A^-A}$ at each solvent composition. This was done for both the measured and statistical (non-cooperative) value. Species concentrations and standard errors are tabulated in Table 4.

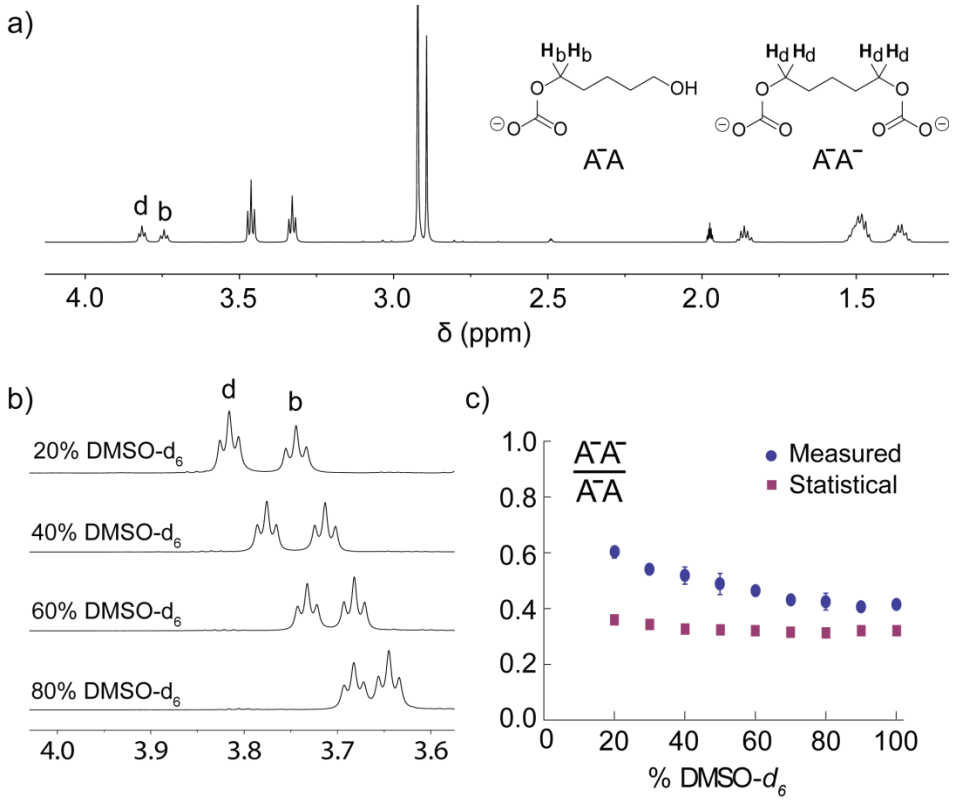

Figure S10. Solvent titration experiment. a) ^{1}H NMR spectrum indicating diagnostic signals (H_d and H_b), which were used to calculate the ratio $\frac{A^-A^-}{A^-A}$. b) ^{1}H NMR spectra of H_d and H_b at various solvent compositions. c) The ratio $\frac{A^-A^-}{A^-A}$ plotted against solvent composition. Blue circles indicate the measured ratio, while purple squares indicate the statistically expected ratio (if there was no proximity effect).

%DMSO-d_6	AA_i (mM)	A^-A^- (mM)	A^-A (mM)	AA_f (mM)	p	A^-A^-/A^-A		A^-A^-/A^-A (avg. ± std. dev)	
						Measured	Expected	Measured	Expected
20	102	24	38	41	0.42	0.63	0.36	0.60±0.02	0.36±0.00
	101	23	39	40	0.42	0.59	0.36		
	98	22	38	38	0.42	0.59	0.36		
30	103	22	39	42	0.40	0.55	0.34	0.54±0.01	0.34±0.00
	97	20	38	38	0.41	0.53	0.34		
	106	22	42	42	0.41	0.53	0.34		
40	96	19	37	40	0.39	0.52	0.32	0.52±0.03	0.33±0.01
	106	20	42	44	0.39	0.49	0.32		
	103	21	39	42	0.40	0.55	0.33		
50	104	19	41	43	0.38	0.47	0.31	0.49±0.04	0.32±0.01
	103	19	42	42	0.39	0.47	0.32		
	104	21	40	43	0.40	0.53	0.33		
60	99	18	39	42	0.38	0.46	0.31	0.46±0.00	0.32±0.01
	100	19	41	40	0.39	0.46	0.32		
	96	18	39	39	0.39	0.47	0.32		
70	98	17	40	41	0.38	0.43	0.31	0.43±0.01	0.31±0.01
	98	17	41	40	0.39	0.42	0.31		
	100	18	41	40	0.39	0.44	0.32		
80	100	18	40	42	0.38	0.45	0.31	0.42±0.03	0.31±0.01
	100	17	43	40	0.38	0.39	0.31		

	104	19	44	41	0.39	0.43	0.32		
90	103	18	43	43	0.38	0.41	0.30	0.40±0.01	0.31±0.01
	105	19	45	42	0.39	0.41	0.32		
	104	18	45	41	0.39	0.39	0.32		
100	108	19	46	43	0.39	0.42	0.32	0.41±0.01	0.32±0.00
	104	18	45	41	0.39	0.40	0.32		
	99	17	42	40	0.39	0.42	0.31		

Table S6. Tabulated data for the solvent titration.

Effective Molarity (EM) Titration

Samples for this titration experiment were prepared and spectra acquired and processed in the same manner as described above (see *Solvent Titration*), except for this titration AA_i was varied (50 mM and 200 mM, ~25 mM increments) at each solvent composition from 20%-100% DMSO-d_6. Increasing AA_i, and therefore AA_f, biases the equilibrium towards the monoalkylcarbonate A^-A. Intuitively, this is because the complex $G^+G^+:A^-A^-$ depends linearly on AA_f, while $G^+G^+:(A^-A)_2$ depends on the square of AA_f. Thus, increasing AA_f favors the monoalkylcarbonate A^-A over bisalkylcarbonate A^-A^-. ^{1}H NMR spectra were recorded following equilibration under 1 atm CO_2. For each sample, the ratio $\frac{A^-A}{A^-A^-}$ was calculated and plotted against the final, unreacted diol concentration AA_f. Note that the ratio $\frac{A^-A}{A^-A^-}$ is the reciprocal of that used in the previous solvent titration plots. This is done to linearize the data (see equation 10, derived below) and allow quantification of EM (effective molarity). $AA_f$was determined by integrating the resonance between 3.35 ppm to 3.50 ppm corresponding to protons adjacent an unreacted alcohol group. Note that this signal includes contributions from both AA_f and A^-A. The contribution from the latter must be subtracted, and can be determined from the downfield signal (H_b) also corresponding to A^-A, as these are equal in area. This signal generally falls between 3.75-3.60 ppm, depending on the solvent composition. At each solvent composition, the plot yielded a strongly linear correlation. The data points were fitted by linear regression and EM determined from equation 10. The EM values were plotted versus solvent composition to obtain Figure 10d.

Derivation of Equation 10

We derive expressions for A^-A and A^-A^- in terms of K_0 and $_{CO_2}$:

$$A^-A = 2\,G^+G^+{:}\,(A^-A)_2 + G^+G{:}\,A^-A$$

Where $G^+G{:}\,A^-A = 4\,GG_f\,AA_f\,K_0\;_{CO_2}$ and $G^+G^+{:}\,(A^-A)_2 = 2\,GG_f\,AA_f^2\,K_0^2\;{}^2_{CO_2}$

and

$$A^-A^- = G^+G^+{:}\,A^-A^-$$

Where $G^+G^+{:}\,A^-A^- = 2\,GG_f\,AA_f\,EM\,K_0^2\;{}^2_{CO_2}$

Next, we solve for the ratio $\frac{A^-A}{A^-A^-}$ to obtain equation 10.

$$\frac{A^-A}{A^-A^-} = \frac{2\,G^+G^+{:}\,(A^-A)_2 + G^+G{:}\,A^-A}{G^+G^+{:}\,A^-A^-}$$

$$\frac{A^-A}{A^-A^-} = \frac{4\,GG_f\,AA_f^2\,K_0^2\;{}^2_{CO_2} + 4\,GG_f\,AA_f\,K_0\;_{CO_2}}{2\,GG_f\,AA_f^2\,EM\,K_0^2\;{}^2_{CO_2}}$$

$$\frac{A^-A}{A^-A^-} = \frac{2\,AA_f}{EM} + \frac{2}{EM\,K_0\;_{CO_2}}$$

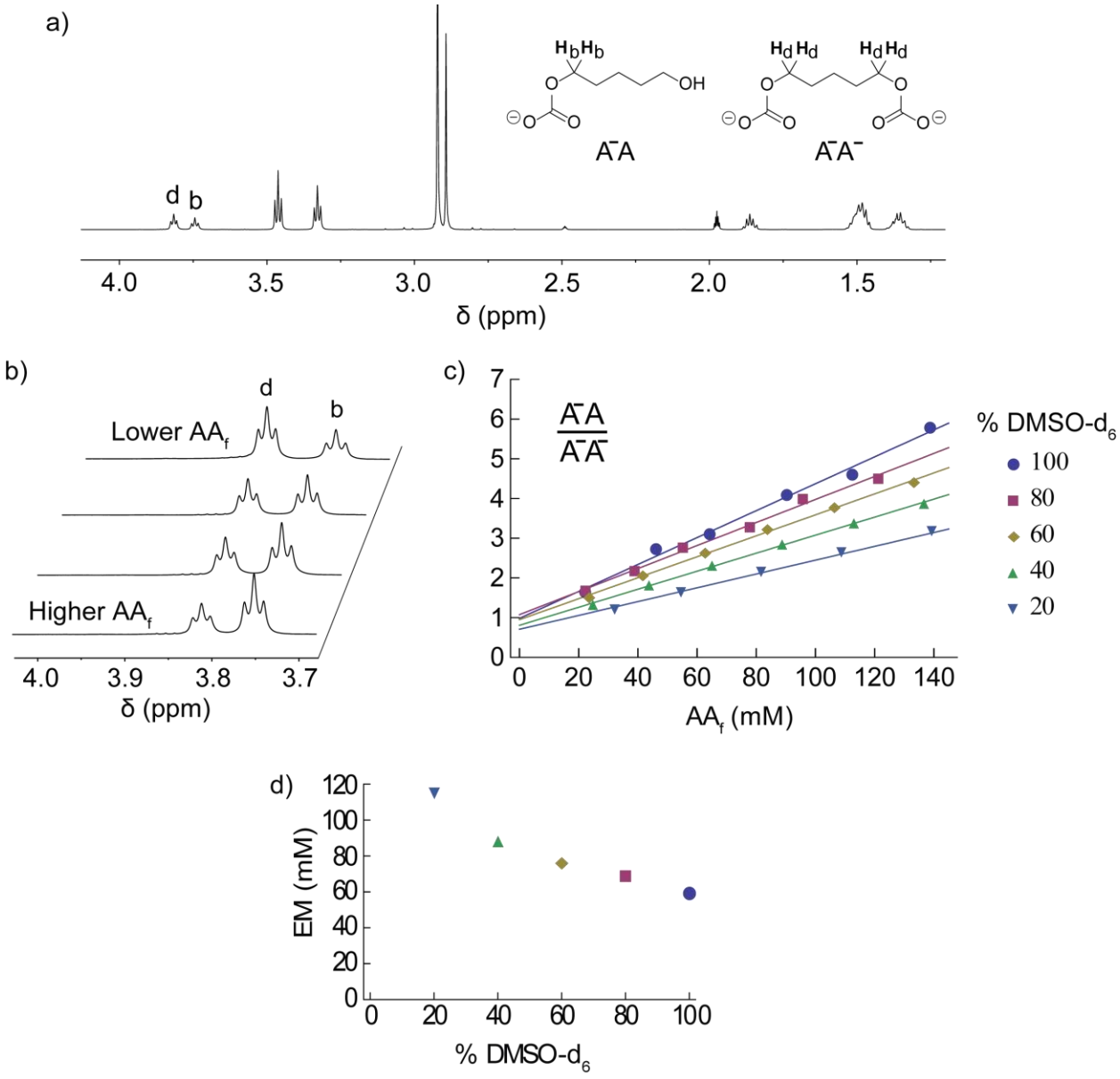

Figure S11. *EM* titration experiment. a) ^{1}H NMR spectra after CO_2 exposure. Diagnostic signals corresponding to monoalkylcarbonate A^-A (H_b) and bisalkylcarbonate A^-A^- (H_d) are labeled. The integration of H_b and H_d was used to calculate the ratio $\frac{A^-A}{A^-A^-}$. b) Relative peak areas of H_b and H_d at varying concentrations of AA_f. c) The ratio $\frac{A^-A}{A^-A^-}$ versus AA_f at various solvent compositions between 20-100% DMSO-d_6. d) *EM* determined using Equation 10 and plotted versus solvent composition.

%DMSO-d_6	[A$^-$A$^-$]	[A$^-$A] (mM)	[AA]$_f$ (mM)	[A$^-$A]/[A$^-$A$^-$	linear fit

	(mM)			]	
20	26.0	31.1	26	1.20	y=0.024x+0.614
	24.1	39.9	44	1.65	
	21.6	47.2	66	2.19	
	19.6	52.6	87	2.69	
	17.7	57.3	112	3.23	
40	23.1	30.4	20	1.32	y=0.028x+0.791
	21.9	39.5	36	1.81	
	20.1	46.5	54	2.32	
	18.5	52.4	74	2.83	
	16.9	56.8	94	3.36	
	15.3	59.9	113	3.90	
60	21.3	32.1	20	1.51	y=0.032x+0.888
	19.9	41.0	36	2.05	
	18.2	47.9	54	2.63	
	16.7	53.6	73	3.21	
	15.1	57.7	92	3.83	
	13.9	62.5	114	4.49	
80	19.8	34.1	22	1.72	y=0.036x+0.884
	20.4	45.5	38	2.23	
	17.2	48.7	55	2.83	
	14.7	50.5	73	3.44	
	13.0	55.7	93	4.30	
	11.7	59.0	115	5.03	
100	20.2	33.2	18	1.65	y=0.041x+0.977
	16.1	43.7	38	2.72	
	16.8	52.1	54	3.11	
	13.6	55.4	75	4.08	
	13.4	61.6	94	4.60	
	10.9	63.0	116	5.79	

Table S7. Tabulated data for the effective molarity titration.

Water Titration

In monodentate systems, water is known compete against alcohols for CO_2 binding, forming bicarbonate rather than alkylcarbonate salts. To test the effect of water in the context of a bidentate system, we performed a water titration experiment in which solvent composition (20% DMSO-d_6), and the concentration of GG (56 mM) and AA (83 mM) (initial concentrations) were kept constant, while the concentration of H_2O (0-220 mM) was varied. As the water concentration increases, we observed the concentrations of A^-A and A^-A^- decrease but the concentration of AA_f increase, although the combined concentration of all three species remains roughly constant. Additionally, we observed that the total concentration of guanidine species (GG_f, G^+G, and G^+G^+) decreases, concomitantly with the appearance of a white precipitate when the concentration of $H_2O \geq 55$ mM. These observations are consistent with H_2O out-competing AA for CO_2 binding to form bicarbonate salts. As the H_2O concentration increases, bicarbonate formation biases the equilbirum away from alkylcarbonate formation, causing A^-A and A^-A^- to revert back to AA. Bicarbonate formation also explains the decrease in guanidine species in solution through the precipitation of the guanidinium-bicarbonate salt.

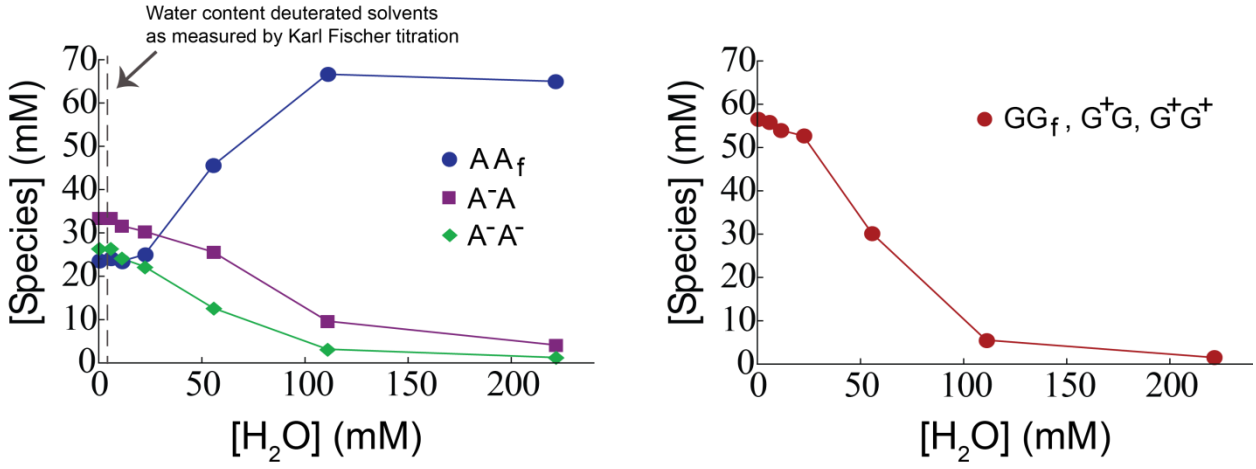

Figure S12. Species concentration as a function of [H_2O].

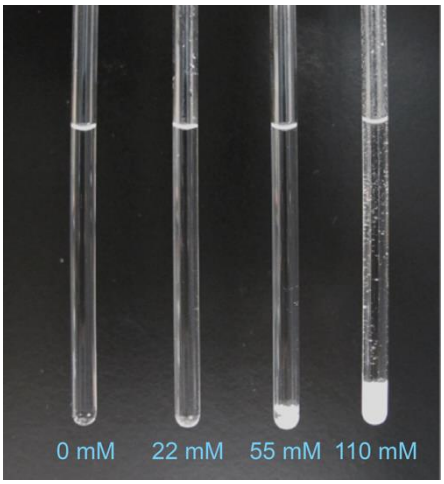

Figure S13. White precipitate was observed for NMR samples with the concentration of $H_2O \geq 55$ mM.

V. References

1) Hunter, C.A.; Anderson, H.L. What is Cooperativity? *Angew. Chem. Int. Ed.* **2009**, *48*, 7488-7499.
2) Heldebrant, D.J., Yonker, C.R.; Jessop, P.G.; Phan, L. Organic Liquid CO_2 Capture Agents with High Gravimetric CO_2 Capacity. *Energy Environ. Sci*. **2008**, *1*, 487-493.